

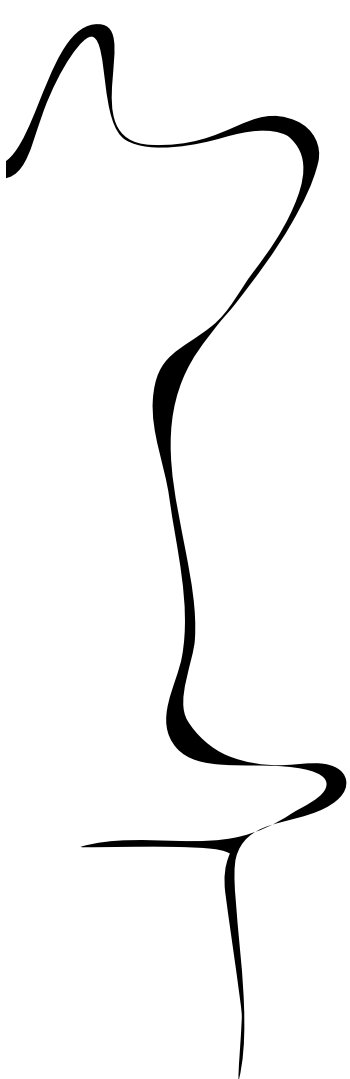
Bachelor thesis Biomedical Technology

Light fluence marker for quantitative photoacoustic imaging

Cas Weernink

Bachelor Student Biomedical Technology

S2392364



Biomedical Photonic Imaging

Chairman:	prof.dr.ir. W. Steenbergen
Daily supervisor:	F. Kalloor Joseph PhD
External member:	B. De Santi PhD

Date

July 15, 2022



UNIVERSITY OF TWENTE.

1 Abstract

Carotid atherosclerosis is a disease in which the carotid artery narrows down due to plaque formation. Photoacoustic imaging is a promising technique for providing information about the plaque composition. In this research, it is studied if photoacoustic imaging can be used to obtain the absorption spectrum of an unknown absorber. Furthermore, the relation between the concentration of the chromophore and the resulting photoacoustic signal is investigated. This study is based on a hypothesis that a known absorber can be used to correct for the difference in light propagation at different wavelengths, to retrieve the absorption spectra of an unknown chromophore. In the experiment, two tubes containing a solution of India Ink are examined. The tubes are examined with multiple wavelengths of light and the measured PA signals of one tube are compensated for the differences in the signal from the other tube, which has a constant, known concentration ink. The resulting photoacoustic signal follows the absorption spectrum of India Ink. The relation between the photoacoustic signal and the concentration of the chromophore is not linear proportional. Looking at the amount of signal coming from across the tube might give an indication about the light fluence at that particular depth.

Contents

1	Abstract	1
2	Introduction	3
2.1	Quantitative Photoacoustic Imaging	4
2.2	Relation between concentration and photoacoustic signal	5
3	Research question and hypothesis	6
3.1	Goal	6
3.2	Hypothesis	6
3.3	Research questions	6
4	Experimental set up	7
4.1	Production of five India Ink Dilutions	7
4.2	Requirements, experimental set up and protocol	9
4.3	Protocol using set up	11
4.3.1	Start up system	11
4.3.2	Shut the system down	12
4.4	Protocol doing a measurement	13
4.4.1	Data processing	15
4.5	Results	16
5	Analysis of the gained data	18
5.1	Profile plots	18
5.2	Pulse energy compensated	26
5.3	Compensating for difference in reference tube	28
5.3.1	Results for photoacoustic signal versus wavelength	29
5.3.2	Actual versus estimated μ_a values	33
5.3.3	Concentration versus estimated μ_a values.	33
6	Conclusions and recommendations	37
7	Outlook	38
8	Appendix	40
	Appendix I. Pulse energies for different wavelengths	40
	Appendix II. IMA_C5_3_PA_standAlone_avg MATLAB script.	41
	Appendix III. MATLAB-script for reconstructing the photoacoustic image.	48
	Appendix IV. MATLAB-script for obtaining the average PA signal of the ROI.	50
	Appendix V. MATLAB-script for analysing the data and obtaining all the plots.	52

2 Introduction

Carotid artery stenosis or carotid artery disease is the medical condition in which the carotid artery narrows down due to plaque formation on the inside of the blood vessel, as shown in Figure 1.

The obstruction of the artery increases the risk of a stroke, which is the second leading cause of death worldwide. [2] In an early stage, the disease might be unnoticed as long as enough blood is provided to the brain. When the artery is narrowed down in such a way that this is not the case anymore, people will suddenly have problems with speaking and seeing and will experience weakness and numbness on one side of the body. A stroke can be caused by a plaque in two ways. One is when the plaque obstructs the carotid artery in such a way that the brain is not receiving enough blood. The other one is when a piece of the plaque comes loose and blocks a smaller blood vessel higher in the brain. Current imaging techniques only allow examination of the dimensions of the plaque and not its composition. The plaque consists of multiple substances such lipids, blood and collagen and the specific composition determines the vulnerability and stability of the plaque.[3] It is therefore desired to have a method for determining the concentrations of those components, because then it will be better possible to do a risk analysis and to apply the best possible treatment. Photoacoustic (PA) imaging is a promising, relatively new, imaging technique which can provide information on the concentrations of certain substances.

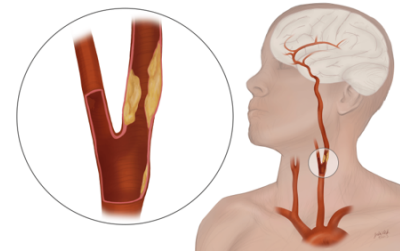


Figure 1: Plaque formation in the carotid artery. [1]

The technique uses the advantages of both optical imaging and ultrasound (US). In PA imaging, light with a specific wavelength is sent into a sample, where different chromophores will absorb the light in different ways, due to their differences in absorption spectra. When the light is absorbed, the chromophore will slightly heat up, causing the pressure to rise, resulting in the production of an US wave. This wave propagates back through the sample to a probe where an array of transducer elements measure the signal. When the speed of sound in the sample is known and multiple transducer elements measure the signal, it is possible to find the location of the source of the signal by using for instance backprojection.

Optical imaging is characterised by the capability of imaging with a high contrast, since every substance has different absorption characteristics for different wavelengths. For most optical imaging techniques, light has to be ballistic, meaning that the scattering of light limits the possible depth of imaging which results in low imaging depths. A US wave can propagate further distances through a sample without being influenced. The transducer only measures the US wave and therefore it is not necessary that the light is ballistic. The result of this is that the light can travel deeper and still generate a clear signal. So by combining both techniques, PA imaging is a very promising technique for measuring the presence of certain substances in a sample.

For clinical usage, PA imaging could be used to examine the presence of tumor cells, to measure the blood oxygen saturation and also to investigate the presence of substances as lipids in a plaque. To be able to determine the amount of those substances present in a sample, quantitative photoacoustic imaging (QPAI) can be used. This technique uses multiple wavelengths of light to obtain multiple images, from which accurate estimations can be made for the concentration of chromophores such as lipids present in a sample with other scattering and absorbing substances present.

2.1 Quantitative Photoacoustic Imaging

As discussed above, PA images consist of measured ultrasound waves which are produced by the absorption of light by chromophores. In this section it will be briefly discussed how PA waves are generated, how image reconstruction can be done and what the principle is of QPAI.

For photoacoustic imaging, mostly light in the near infrared (NIR) range is used. This light is non ionizing and the absorption of water and the scattering of tissue is low and permits therefore deeper tissue penetration. The photoacoustic signal is produced by the absorption of the light by chromophores. This process of absorbing a photon, generating an increase in pressure due to the increase of temperature, and then the propagation of an ultrasound wave is called the photoacoustic effect. The relation between the initial pressure that is created at a point r ($P_0(r)$) and the absorbed energy density at that point $H(r)$ may be written as

$$P_0(r) = \Gamma H(r) \quad (1)$$

where Γ is the Grüneisen coefficient, a constant which gives the efficiency of heat to pressure conversion, which is given by $\Gamma = \beta c^2 / C_p$, with β being the volume thermal expansivity, c the speed of sound and C_p the heat capacity at constant pressure.

The absorbed energy density is depended on the absorption coefficient (μ_a), and the light fluence (ϕ) and is given by

$$H(r) = \mu_a(r, \lambda) \phi(r, \lambda, \mu_a, \mu_s) \quad (2)$$

where λ is the wavelength of the light and μ_s is the scattering coefficient.

All this can be rewritten into the final expression

$$P_0 = \Gamma \mu_a(r, \lambda) \phi(r, \lambda, \mu_a, \mu_s) \quad (3)$$

Reconstruction of a photoacoustic image is done by backprojection of the received signal. In Figure 2 this principle is shown. Every detector element measures the pressure wave coming from a chromophore absorbing the light. All the elements detect the signal at another time, due to the difference in distance to the source. By knowing the speed of sound in the sample and the time between the light being pulsed and receiving the signal, it's possible to determine for every element a circular region on which the source should be located. By overlapping all the circles for the different elements, the spot can be found that lays on the circle of every element. In this way, the location where P_0 was generated can be found. There are multiple detector geometries, but this research is focused on a planar geometry, since for spherical or cylindrical geometries, all points around the sample should be accessible, which is not the case for the carotid artery. The backprojection can be done by taking the Fourier transform of the measured time-dependended pressure data across the surface, then mapping the temporal frequency to the axial spatial frequency and finally taking the inverse Fourier transform to get P_0 . [4]

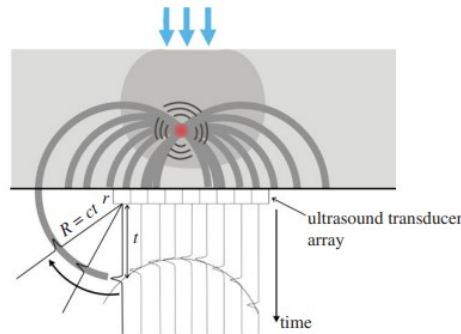


Figure 2: Principle of reconstructing a photoacoustic image using backprojection. [5]

2.2 Relation between concentration and photoacoustic signal

Literature states that the image contrast is mostly determined by optical absorption.[5] Here it is important to state that this does not mean that the PA signal is directly proportional to the absorption coefficient μ_a . As can be seen in Eq. 3, P_0 is proportional to μ_a and to ϕ , which is also depended on μ_a , meaning that the PA signal is not linear proportional to only the absorption coefficient.

According to literature [6, 7], when cylindrical objects are investigated, such as blood vessels or tubes, there are some circumstances where the light fluence is known and where the assumption can be made that the influence of the absorption coefficient on that light fluence can be neglected. In those situations a linear relation is seen between the light absorption coefficient and the PA signal amplitude. There are two cases in which this holds. One being the situation in which the blood vessel, or a tube in the case of this experiment, has such a small radius that it satisfies Eq. 4. In the second case, the relation can also be linear for larger tubes if the central frequency of the transducer is high enough to fulfil the first criterion showed in Eq. 5 and when μ_a satisfies the second criterion.

$$\mu_a a \ll 1 \quad (4)$$

$$a \gg \Lambda \quad \wedge \quad \mu_a < 1/\Lambda \quad (5)$$

Where a is the radius of the blood vessel and Λ is the ultrasonic wavelength corresponding to the central frequency of the transducer. In Figure 3, the relation between photoacoustic signal and the absorption coefficient is shown. Here it is clearly depicted that there exist a linear and a non linear region. This figure is originating from the paper of Mathangi Sivaramakrishnan et al.[7]

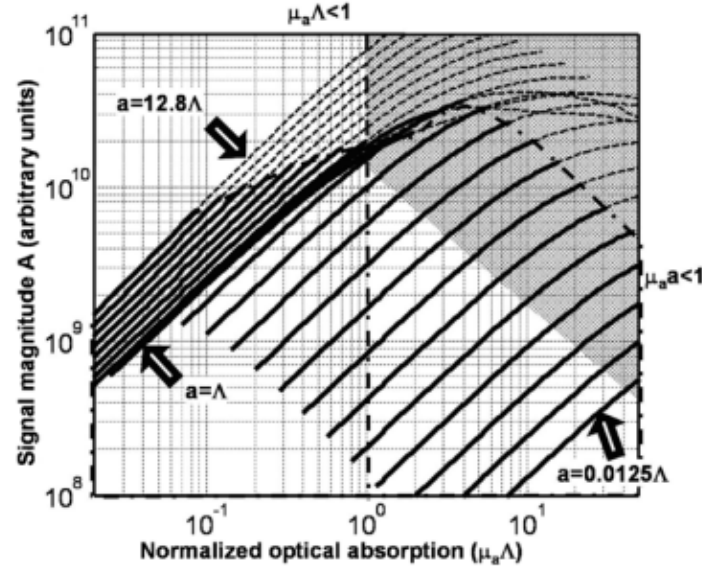


Figure 3: Magnitude of the photoacoustic signal as a function of the optical absorption coefficient normalised by the acoustic wavelength ($\mu_a\Lambda$) for different normalised cylinder radii. The non-shaded region indicates the circumstances under which the PA signal is linear depended on the absorption coefficient. The shaded region is the part where this relation is not linear. Figure originating from the paper of Mathangi Sivaramakrishnan et al.[7]

3 Research question and hypothesis

3.1 Goal

Before it is possible to quantify an unknown concentration of lipids within the carotid artery, it is necessary to investigate if photoacoustic imaging is capable of providing this information. In this study this is studied for a simplified situation, in which India Ink is located in a tube within a bin of water and intralipids. The goal of the study is to use a known concentration of India Ink as a reference to quantify unknown concentrations of India Ink. This is done by analysing the relation between the photoacoustic signal coming from the tube and the absorption spectra of the different concentrations of India Ink.

3.2 Hypothesis

When an India Ink solution with a μ_a is placed within a tube with a inner radius of such a dimension that $a \gg \Lambda$ is true, than a linear relation is expected, according to the literature that is stated in Paragraph 2.2. The transducer that is used in this study has a central frequency of 5 MHz. With a taken value for the speed of sound of 1485 m/s, corresponding to the speed of sound in water and intralipids, the central wavelength has a value of 0.297 mm. Following the condition given in Eq. 5, μ_a should be smaller than $1/(0.297) = 3.37 \text{ mm}^{-1}$. When India Ink solution are used with absorption coefficients similar to that of oxidised blood, which is $\mu_a = 0.38 \text{ mm}^{-1}$ at a wavelength of 800 nm[8], this will be the case. Because of this, a linear proportional relation is expected. This means that if two solutions with C_1 and $C_2 = 2 * C_1$ are investigated for a specific wavelength, a PA value twice as high is expected for C_2 compared to C_1 .

Furthermore, when looking at the PA values coming from a specific concentration looked over a range of wavelengths, it is expected that the corresponding graph has the same shape as the absorption spectrum.

3.3 Research questions

The following research questions stand central in this study.

Using the theoretical background as mentioned above, combined with prior knowledge about the optical properties of a known chromophore (in this study India Ink), is it possible to:

- (i) Study the nature of the fluence at a specific location?
- (ii) Obtain the absorption spectra of an unknown chromophore, without knowing the fluence variations and laser pulse energy?
- (iii) Obtain the relation between the concentration of a chromophore and the photoacoustic signal, eliminating other variables?

4 Experimental set up

In this chapter the experimental set up and the measurement methods are explained. The aim of the experiment is to image two tubes containing India Ink solutions, one being a reference tube containing a constant concentration of India Ink and one being a test tube in which five different concentrations of India Ink are investigated.

The following sections are present:

- (i) Production of five India Ink Dilutions.
- (ii) The experimental set up.
- (iii) Protocol on how to use the photoacoustic imaging system and a protocol on how to do the measurements.
- (iv) Post processing method to properly analyse the data received from the PA measurements.

4.1 Production of five India Ink Dilutions

When India Ink is purchased, the concentration of the stock solution is unknown, meaning that it is not possible to express the concentration of India Ink in a form of moles/litre. Following Beer Lambert law, there is a linear relationship between the absorbance (and thus the absorption coefficient) and the concentration of a substance. A spectrophotometer can measure the absorbance of a dilution in the UV/VIS range of wavelengths. In the rest of this report, the concentrations of different dilutions are expressed in the form of μ_a (mm^{-1}) for light with a wavelength of 800 nm.

Seven dilutions were made by adding a certain amount MilliQ water to a certain amount of India Ink stock solution. Eventually the different ratios of India Ink stock solution : MilliQ water lay in a range of 1:500 to 1:8000. In Table 1, the different ratios and how they were produced are shown.

Dilution India Ink : MilliQ water	Amount of India Ink (μL): MilliQ (mL)
1 : 500	200 : 100
1 : 750	133 : 100
1 : 1000	100 : 100
1 : 1500	67 : 100
1 : 2000	50 : 100
1 : 4000	25 : 100
1 : 8000	12.5 : 100

Table 1: Different dilutions of India Ink and how they are produced

After making the dilutions, the absorbance was measured with the spectrophotometer. The spectrophotometer measures the amount of light reaching the detector behind the sample. In other words, it measures how much light is absorbed by the sample. According to the user instruction of the spectrophotometer, the spectrophotometer gives trustworthy results as long as the absorbance of the sample is not much higher than 1.00 absorbance unit (AU). Using Eq. 6 corresponding to a absorption coefficient of $\mu_a = 0.23 \text{ mm}^{-1}$.

To measure the absorbance of the different dilutions, a small amount of all the solutions was further diluted to get a dilution ratio of 1:6000, after which the absorbance was measured three times for every 1:6000 dilution. The obtained absorption spectra are showed in Figure 4 Since the absorbance and concentration are linear related, the absorbance of the original dilution can

be calculated. With Eq. 6, in which d is the path length of the light through the sample (in this case a 10 mm cuvette), the absorption coefficient for specific wavelengths can be calculated.

$$\mu_a = \frac{\ln(10^{\text{absorbance}})}{d} \quad (6)$$

In Table 2, the averaged absorbance values (over three measurements for the 1:6000 dilutions), the calculated absorbance for the stock dilution and the corresponding absorption coefficients are shown for a wavelength of 800 nm.

It can be seen that the dilutions in the range of 1:500 - 1:2000 have approximately the same average absorbance value for the further diluted 1:6000 dilutions. The absorbance measured for the further diluted 1:4000 dilution is more off. The 1:8000 dilution is not further diluted, but gives a similar absorbance value as the 1:6000 dilutions, where it should give a lower value, around $A = 0.428 \text{ AU}$. These two difference of absorbance values compared to the expected values can be the results of the way of pipetting. India Ink droplets stuck quite easily onto the exterior side of the pipette tip and since for these two dilutions a small amount of India Ink had to be added, a small droplet can have a bigger influence.

The goal was to have at least five solutions with different absorption coefficient close to the one of oxidised blood, which is $\mu_a = 0.38 \text{ mm}^{-1}$ at a wavelength of 800 nm.[8]. Because of this all, the choice is made to only use the dilution with the absorption coefficients $\mu_a = 1.608$, $\mu_a = 1.044$, $\mu_a = 0.814$, $\mu_a = 0.529$ and $\mu_a = 0.391$.

Dilution	Average absorbance 1:6000 ($\lambda = 800 \text{ nm}$) (AU)	Average absorbance stock dilution	calculated $\mu_a \text{ (mm}^{-1}\text{)} \text{ at}$ $\lambda = 800 \text{ nm}$
1:500	0.582	6.984	1.608
1:750	0.567	4.536	1.044
1:1000	0.589	3.534	0.814
1:1500	0.575	2.300	0.529
1:2000	0.566	1.698	0.391
1:4000	0.623	0.935	0.215
1:8000	0.578 (not further diluted)	0.578	0.133

Table 2: Table with the measured average absorbance of the dilutions further diluted to 1:6000, the calculated absorbance for the original dilution and the calculated corresponding μ_a

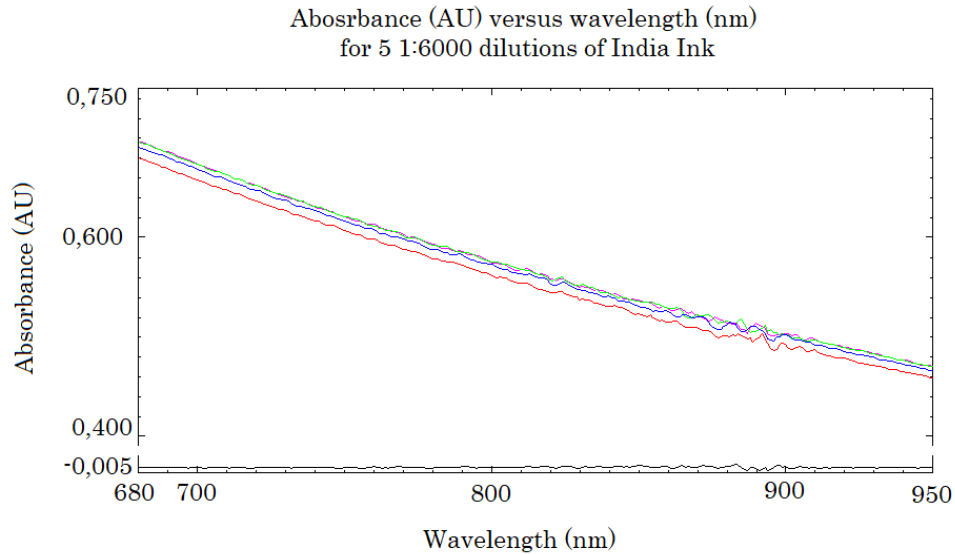


Figure 4: Absorption spectra of five 1:6000 India Ink dilutions, obtained when the five different solutions were further diluted. Spectra obtained using the spectrophotometer.

4.2 Requirements, experimental set up and protocol

In this subsection, the requirements, the experimental step up and the protocol on how to use the set up and how to do the measurements will be discussed.

The experimental set up consists of the following components:

- Q-switched pulse laser
- Opolette 532 laser. Consisting of Quantel Ultra Nd:YAG pump laser and optical parametric oscillator (OPO) technology. From Opotek.
- An objective lens for fiber optic coupling.
- Flip mirror to measure pulse energy.
- Nova II power meter from Ophir.
- Fiber bundle which splits into two bundles ending in two linear laser arrays.
- A concave array ultrasound transducer C5-3, containing 256 transducer elements.
- Two Legion Amp 128-channel preamplifiers from PhotoSound Technologies.
- Vantage 256 system from Verasonics.
- MATLAB
- Intralipid (20%)
- Four 4 mm inner, 8 mm outer radius silicon tubes from Rubber Webshop.
- 3D printed transducer, laser array and tube holder. This is a custom designed holder which is shown in Figure 6.
- India Ink solutions with different concentrations.

Laser light is generated in a Opolette OPOTEK laser, which has a range of laser light of 680 nm - 950 nm. The emission of the laser light is regulated by a Q-switch with a frequency of 20 Hz. The laser light has a varying pulse energy over wavelength, with values between approximately 2.0 - 4.0 mJ. When the laser light is emitted, it is focused in such a way that the diverging light beam after the focus point has exactly the width of the opening of the fiber bundle. This fiber bundle takes up all the laser light and then splits the bundle into two separated bundles. These bundles end each in a different linear laser array, where the light leaves the fiber bundle. These arrays are attached next to a concave transducer probe in a custom designed 3D-printed holder. When doing measurements, this probe holder was placed in a bin filled with water to reduce acoustic impedance and reflection. The sample is placed under the probe holder. This can be done at different locations, giving different results. In this research, only tubes with a liquid solution were examined. The tubes were placed into a 3D printed tube holder, which has 35 places to locate the tubes. This tube holder could then be attached to the probe holder, to ensure a constant set up between the tubes, the laser arrays and the probe. In the way the experiment was executed for this report, a separated tube and probe holder were attached to each other using a clamp and tape, as can be seen in Figure 5. A new design has been made, in which the probe and tube holders are merged into one holder. Figure 6 shows the design in Solidworks. The holder is already printed and available at the Biomedical Photonic Imaging (BMPI) group at the University of Twente.

After receiving the ultrasound wave, the signal acquired by the probe is amplified by two amplifiers and then is digitised by the Verasonics system. A MATLAB script processes the signal to eventually deliver the desired data which can be processed for analysis.

In Figure 5 the experimental set up is shown.

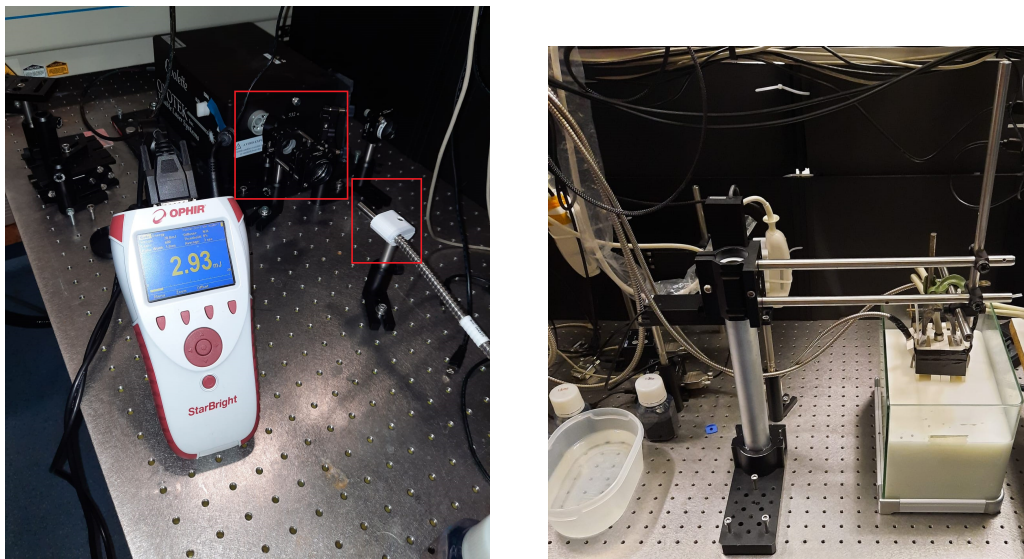


Figure 5: Experimental set up with in (a): Opolette 532 laser emits light into optics, which consist of first a flip mirror and than an objective lens, where the fiber is placed behind. In the front the power meter is visible. In (b): the other part of the set up. The fiber is splitted into two, which enter the probe holder. The probe holder is placed within a bin containing water mixed with 5% intralipids.

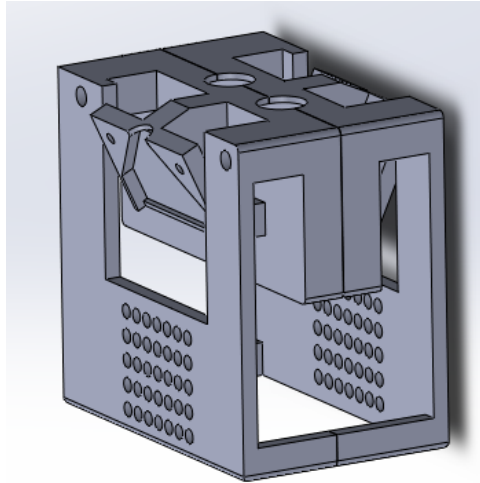


Figure 6: Design of the probe and tube holder combined together.

4.3 Protocol using set up

In this paragraph, a protocol is given on how the experimental set up is used.

4.3.1 Start up system

1. Put on the laser *Interlock*.
2. Start up the laptop which has the OPOTEK user software and the computer on which the Verasonics is connected.
3. Start up the laser cooler.
 - (i) There are two flips on the back side, the bottom one (external trigger) should be flipped to the right.
 - (ii) The pulse repetition rate on the cooler should be set to 00.
4. Turn on the function generator and the laser driver.
 - (i) The laser generator has two output cables, channel 1 is for the flash lamp, channel 2 is for the Q-switch. Both have to be turned on.
 - (ii) Press the recall button and then select the first channel. The frequency should be at 20 Hz and the delay should be 180 microseconds.
In Figure 7, the display with the correct settings can be seen.
5. On the laptop, open the OPOTEK program.
 - (i) At the settings, set both the flash as the Q-switched setting to "External".
 - (ii) Set the intensity to 100.
6. Start MATLAB, go to "Vantage" folder and open the IMA_C5_3_PA_standAlone_avg code. This is a custom developed program by the BMPI group of the University of Twente for photoacoustic imaging using the concave ultrasound transducer C5-3. The script can be found in Appendix II.
 - (i) Run the command *activate* in the command window and click accept.
 - (ii) Run the script.

- (iii) Run the command *VSX* in the command window
- (iv) Select the .mat - file with the same name as the script by using the arrow keys.
- 7. Put on the correct safety goggles.
- 8. Close the curtains of the compartment.
- 9. Turn on the amplifiers.
Important! From this point on it is only allowed to run scripts specifically made for photoacoustic imaging. With scripts for ultrasound, the amplifiers can be damaged.
- 10. Finalise the set up, e.g. place the tubes with the sample and the transducer within a bin of water.
- 11. Set the laser to the desired laser wavelength via the OPOTEK software on the laptop and start the laser.
- 12. Execute the desired measurement.
Saving the data can be done by *Freezing* the live image on the control screen on the computer where MATLAB is running. Then save the RF file on the computer.

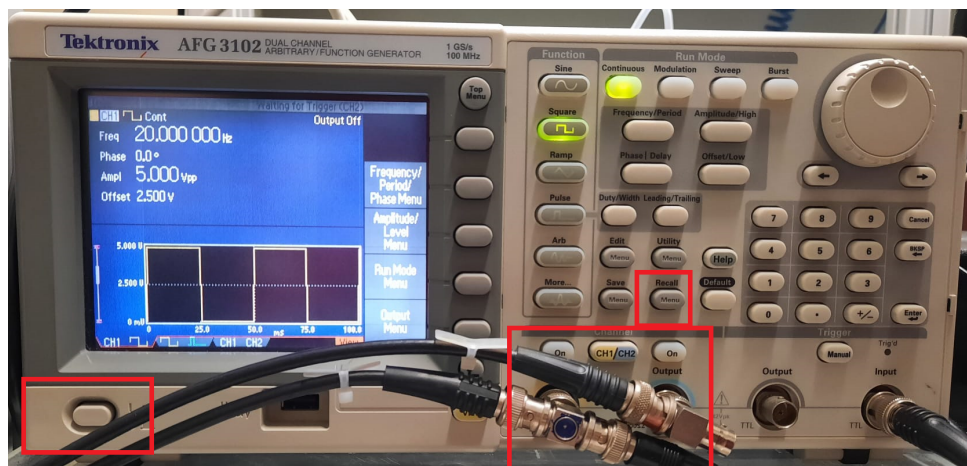


Figure 7: The correct settings for the laser driver. The button marked on the bottom left is the power button and in the middle of the bottom two "On" buttons should be pressed in and give light. The display shows the right settings, these can be obtained by pressing the button "Recall", which is marked in the Figure.

4.3.2 Shut the system down

- 1. Shut down the MATLAB script by first closing the control panel and then the live visualisation screen.
- 2. Shut down the laser via the laptop.
- 3. Shut down the OPOTEK program first! Do this before shutting down the laser cooler, otherwise the calibration of the laser can be ruined.
- 4. Shut down all the machines by flipping the knobs.
- 5. Shut down the Verasonics and the computer, for the laptop only the screen has to be closed.

6. Shut down the power supply to the amplifiers, otherwise they might burn out.
7. Remove the transducer probe out of the bin of water and clean up the workspace.
8. Turn off the Interlock.

4.4 Protocol doing a measurement

In this paragraph it is concise described how the measurements were done.

1. Fill the bin with 5 litres of water
2. Add 250 mL (5%) intralipids. This mimics the scattering behaviour of tissue.
3. Place one tube at the first row (24 mm depth) and third column and one tube at the first row and fifth column in the tube holder.
4. Fill the tube at the fifth column with the $\mu_a = 0.391 \text{ mm}^{-1}$ for $\lambda = 800 \text{ nm}$ India Ink solution. This tube will always contain the same concentration of India Ink and will be used as the reference sample. From now on, this tube will be referred to as the reference tube.
5. Fill also the tube at the third column with the $\mu_a = 0.391 \text{ mm}^{-1}$ for $\lambda = 800 \text{ nm}$ India Ink solution. This tube will be the tube with varying concentrations India Ink during the different measurements. From now on, this tube will be referred to as the test tube.
6. Fix the tubes with the extra 3D printed blocks which can be clinged onto the tubes using screws or fix the tubes by hooking them behind the probe holder.
7. Place the entire tube/transducer holder in the bin of water and intralipids. Make sure that the whole transducer is under water and that there is no air bubble under the transducer. Since it is not possible to see the transducer due to the intralipids, splash some water against the downside of the transducer. Before doing the first measurement, look if the PA image is as expected.
8. Start the laser and set it to a wavelength of 680 nm. Let the laser emit light for circa 10 minutes.
9. Start up the power meter, make sure the settings are as shown in Figure 8. Dependent on the pulse energy, select the range 2.0 or 20.0 mJ. Change the laser setting according to the wavelength of the laser which is used.
10. Shut down the laser, flip the mirror before the laser beam and start the laser again.
11. Wait until the pulse energy value which is displayed is approximately constant and note this value.
12. Shut down the laser, flip the mirror away from the laser beam and start the laser again.
13. Safe the RF data from the Verasonics by freezing the live image.
14. Repeat step 10 - 13 for seven other wavelengths in the following range: [710 nm, 740 nm, 775 nm, 795 nm, 820 nm, 850 nm, 900 nm].
15. Carry out step 10 - 14 in total three times, such that the experiment is triplicated.
16. Remove the transducer from the bin of water.

17. Remove the tubes from the probe holder and flush out all the ink. Rinse the tubes with water and make sure that the ink is fully removed. Then dry the tubes by blowing air through them.
18. Place the tubes back in the same place. Put again the $\mu_a = 0.391 \text{ mm}^{-1}$ for $\lambda = 800 \text{ nm}$ India Ink solution in the reference tube.
19. Put now the next lowest concentration of India Ink in the test tube. Eventually the following five solutions have to be examined: $[\mu_a = 0.391 \text{ mm}^{-1}, \mu_a = 0.529 \text{ mm}^{-1}, \mu_a = 0.814 \text{ mm}^{-1}, \mu_a = 1.044 \text{ mm}^{-1}, \mu_a = 1.608 \text{ mm}^{-1}]$.
20. Fix the tubes.
21. Repeat step 9 - 20 for all the concentrations.
22. Now all the measurements are done for the tubes located at 24 mm depth, the same steps have to be carried out for the tubes located at 39 mm depth. Place the test tube in the fifth row and third column and the reference tube in the fifth row and fifth column in the tube holder.
23. Repeat step 4 - 21.



Figure 8: Settings for the power meter.

4.4.1 Data processing

The Verasonics obtains the digitised Radio Frequency (RF) data corresponding to each measurement. This data is first filtered with a bandwidth filter with cutoff frequencies 2 MHz and 6 MHz. By using the properties of the probe, such as number of elements and their dimensions, and the speed of sound, backprojection of the signal is possible, reconstructing an image. Before the image is plotted, a Hilbert transform is applied to envelope the signal. The reconstruction image is a plot of intensity values which are proportional to the initial pressure generated at that specific point in the sample. The values have an arbitrary unit as the acoustic calibration of the system is not performed, but the results can be analysed relatively towards each other. In Appendix III the MATLAB script that generates these PA images is given.

In Figure 9 two photoacoustic images are shown for two different depths, one at 24 mm depth and one at 39 mm depth relatively to the centre of the transducer. The images can be seen as cross sections of the sample, with the transducer located at the top of the image. Two tubes filled with India Ink solutions are visible, with on the left a lower concentration ($\mu_a = 0.391 \text{ mm}^{-1}$ for $\lambda = 800 \text{ nm}$) and on the right a higher concentration ($\mu_a = 1.608 \text{ mm}^{-1}$ for $\lambda = 800 \text{ nm}$). The intensity values of a certain area in the image are considered as the PA values corresponding to that specific area. As mentioned above, these intensity have an arbitrary unit, meaning that if investigating the relation between concentration and PA signal is the goal, multiple measurements should be done to compare the different results relatively to each other.

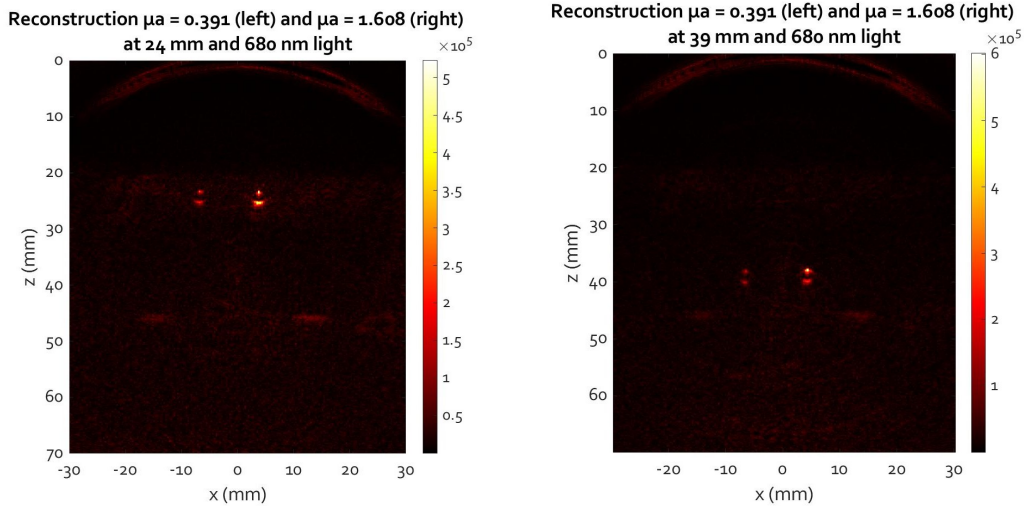


Figure 9: Two photoacoustic images of two tubes with different absorption coefficients located at different depths: left 24 mm depth, right 39 mm depth.

For analysis of the results, a region of interest (ROI) is chosen. This ROI then contains PA values of all the pixels across this area. The average intensity value of this ROI is calculated and is then considered to be the average PA value over the whole tube. As can be seen in Figure 9, not all the pixels across the whole cross section of the tube give a similar PA value. Mostly this is because of two facts. The first one being the fact that a concave ultrasound transducer array is used, which has a limited view angle of 110 degrees, making it impossible to measure the signals coming from the sides of the tubes. The second one is that the transducer is band limited. The transducer has a central frequency of 5 MHz with a bandwidth of 80% which removes the low frequency signals. Therefore the signal coming from inside the tube is not visible.

The calculated average PA value contains a lot of lower noise values and therefore it is not correct to assume that the average PA value is the correct value for the whole tube. However, it is possible to compare different measurements when the same ROI is taken for every measurement and when the assumption is made that the noise has a constant contribution to this average PA

value.

On the basis of one reconstruction image, the centre of the tube is determined. Then a circular ROI is set, which contains the whole tube, as shown in Figure 10. Due to the different proportions of the axis, the circular ROI becomes oval, but since the dimensions of the tube and the white noise are both constant for all the measurement, it does not have an effect on the analysis of the PA values.

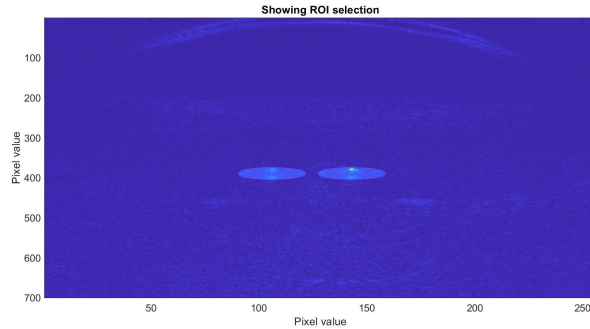


Figure 10: ROI selection for both the reference as the test tube, with the tubes located at 39 mmm depth.

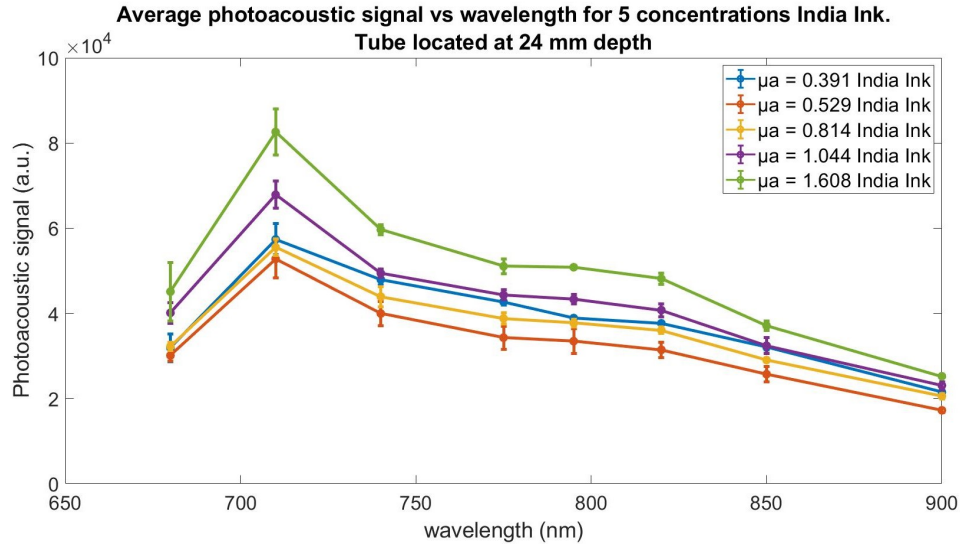
4.5 Results

In Figure 10, the ROI is shown for one measurement with a wavelength of 680 nm. Besides this measurement with laser light of 680 nm, the tube is also emitted with seven other wavelengths: 710 nm, 740 nm, 775 nm, 795 nm, 820 nm, 850 nm and 900 nm. Every measurement, so a single concentration measured for one wavelength, is done three times. In Figure 11 the average of these three PA values of the ROI are plotted against the corresponding wavelength. The errorbars are showing the standard deviation. The results for all the five concentrations of India Ink are shown.

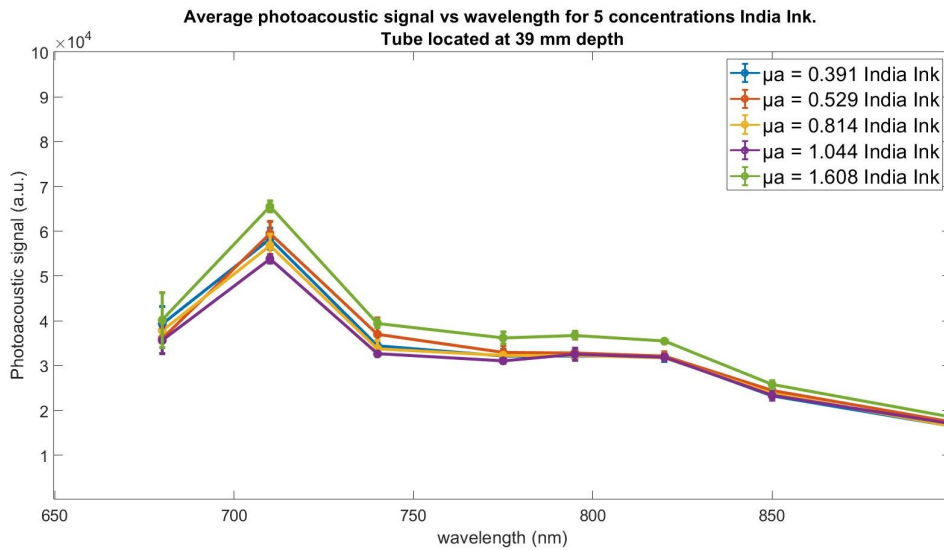
When viewing these result, two things get the attention. First, the photoacoustic signal is not exponentially decaying over wavelength like the absorption spectrum in Figure 4 does. An increase in the PA value at $\lambda = 710 \text{ nm}$ is visible, especially for the tubes at 24 mm depth, and also a increase is seen at $\lambda = 795 \text{ nm}$.

Second, the PA values does not show a linear relation with the concentration of India Ink. When looking at one specific wavelength, for instance 680 nm, the average PA signal is not twice as high for the India Ink with $\mu_a = 1.608 \text{ (mm}^{-1}\text{)}$ compared to $\mu_a = 0.814 \text{ (mm}^{-1}\text{)}$.

In Chapter 5 two different methods are discussed to possibly declare and deal with this.



(a) Photoacoustic signal plotted per wavelength for 5 different concentrations. Tube located at 24 mm depth.



(b) Photoacoustic signal plotted per wavelength for 5 different concentrations. Tube located at 39 mm depth.

Figure 11: Photoacoustic signal plotted per wavelength for 5 different concentrations. PA values are the average of three measurements. Top: tubes located at 24 mm depth; bottom: tubes located at 39 mm depth. The μ_a that are shown in the legends have the unit mm^{-1} and are the values corresponding to $\lambda = 800 \text{ nm}$

5 Analysis of the gained data

In this chapter it is discussed how the gained data from the Verasonics system are analysed and which results are obtained from that.

First, an analysis is done on the photoacoustic signal across a single column of the test tube. So called profile plots show the magnitude of the photoacoustic signal across the vertical cross section of the tube. Then, two different analyse methods are applied to deal with the difference in the received absorption spectra compared to the expected absorption spectrum, as shown in Paragraph 4.4.1. The MATLAB scripts which were used to obtain all the plots that are presented in this chapter can be found in Appendices IV and V.

5.1 Profile plots

In this paragraph, profile plots are shown for the cross section of the tube. The plots display the uncompensated PA values for the specific column in the photoacoustic image which goes through the centre of the test tube. The profile plot is shown for a region starting a view millimeter above the tube and ending a view millimeter below it. There are two types of plots made, one with a constant concentration of India Ink investigated for all the eight different wavelengths, and one for all the five different concentrations of India Ink and a constant wavelength. In Figure 12 the profile plots are shown for the tubes located at 24 mm depth. In Figure 13 the profile plots are shown for the tubes located at 39 mm depth.

In the plots two clear high peaks are visible. These peaks correspond to the signal coming from the ink at the top and bottom part of the tube. The transducer measures a bandlimited signal, where the change in the magnitude of the received ultrasound wave is measured. The entering of the tube produces a high signal, because the intralipids do not absorb much laser light and therefore do not produce a strong US wave, on the other hand India Ink does absorb much light and produces a strong US wave. This change produces the first peak, seen at a vertical depth of 23 mm in Figure 12a. The same holds for the bottom part of the tube. The ink absorbs much light, but the intralipids below it do not. In other words, the change in the magnitude of the US wave that the transducer receives is large, resulting in the second high peak, visible at approximately 25 mm depth in Figure 12. Since the ink absorbs approximately the same amount of light within the tube, the magnitude of the US wave is constant resulting in a low frequency signal which is not measured by the transducer. That is why the photoacoustic signal in that region is low.

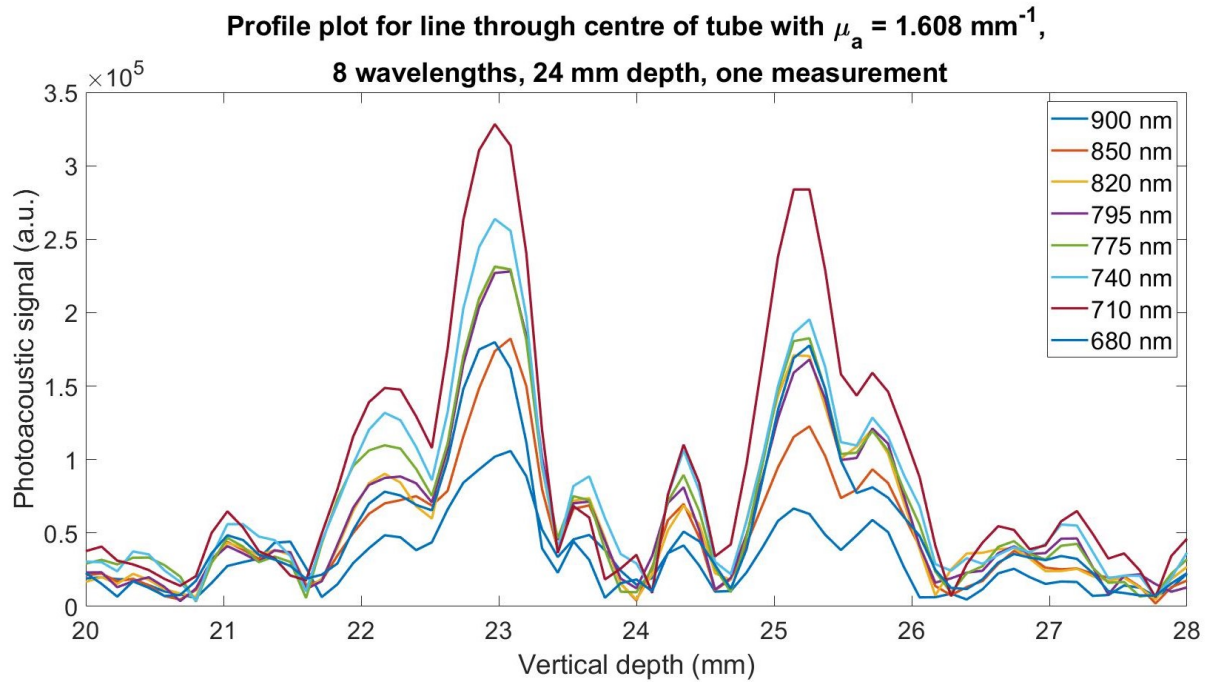
For both Figure 12 as 13, the profile plots for the $\mu_a = 0.391 \text{ mm}^{-1}$ for multiple wavelengths are shown in subfigure a. In subfigure b the profile plots are shown for the five solutions with a wavelength of $\lambda = 820 \text{ nm}$. The profile plots in Figure 12a show two extra, lower peaks before, two within and one behind the tube consistent for all the solutions of India Ink. In Figure 12b, the second peak is higher in value than the first peak for the highest concentration of India Ink. This is unexpected, since light intensity will decay over depth due to absorption and scattering in the sample. The PA images were investigated to see where this is coming from. The results are shown in Figure 14. Subfigure (a) shows a ring artefact above the test tube with two bands with a higher intensity, which can be responsible for the two peak values before the tube. In subfigure (b), a zoomed in image of the test tube $\mu_a = 1.608 \text{ mm}^{-1}$ is shown, which shows that the lateral position of the maximum PA intensity is not the same for the top and bottom part of the tube. For these profile plots column 141 was taken, and in 14 it can be seen that the bottom part has a higher value in this row than the top part of the tube, which explains why the second peak is higher than the first peak in Figure 13 for this concentration.

To take this into account, the profile plots were redone, but than with three columns around the column containing the maximum value. The column containing the maximum value was determined for every measurement separately. The results are shown in Figure 15 and 16.

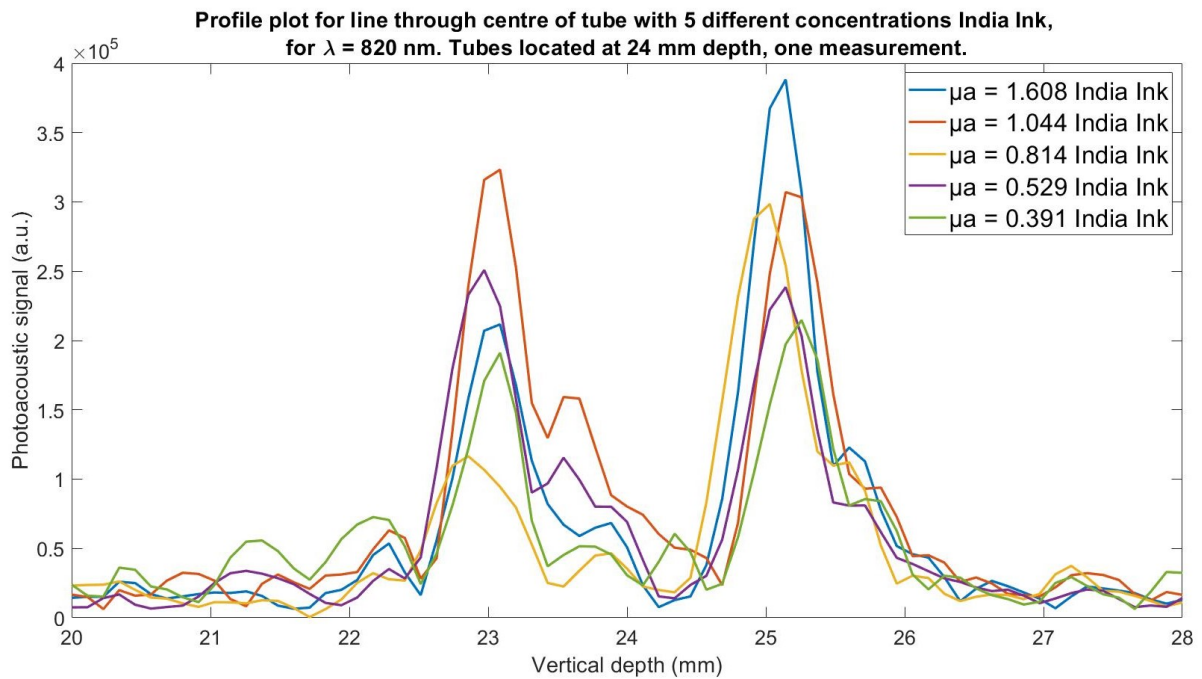
The plots for one concentration over multiple wavelengths are more smoothed out, which is as expected since the average PA values were taken for three columns. In Figure 15 it is visible that the second peak is higher for every measurement. To investigate where this comes from, the photoacoustic images were analysed. Figure 17 shows two PA images of the test tube with $\mu_a = 1.608 \text{ mm}^{-1}$ at $\lambda = 680 \text{ nm}$, located at 24 mm (top) and 39 mm (bottom) depth. In the top figure it is seen that the India Ink gives a much narrower signal at the top of the tube than at the bottom part of the tube, where the signal is broader. This could declare the higher PA value for the second peak, since taking the average of three columns around the column containing the maximum value of the tube gives higher averages for the bottom part than for the top part. In the bottom figure, the test tube is shown when it is located at 39 mm depth. Here it is visible that the top part of the tube gives a broader signal instead of the bottom part, which corresponds to the profile plots where the first peak has a higher value than the second one.

A possible explanation for this result can be the usage of a wrong value for the speed of sound in the reconstruction script. When the actual speed of sound is lower than the one used for the backprojection, the reconstruction of the tube will be fanned out, having a narrow signal for the top part and a broader signal for the part located below that. If a wrong speed of sound was used, it would be expected that for both depths this influence is visible. In other words, also at 39 mm depth the bottom part should give a broader signal than the top part of the tube. Due to light scattering, the light fluence at 39 mm depth is lower than at 24 mm depth, which could declare why this effect is not as clearly visible as at 24 mm depth. However, the note should be made that a wrong value of speed of sound gives indeed a wrong distribution of the PA signal in the reconstruction image, but the total value of the signal should be equal. In other words, the signal can be concentrated in one pixel, or the same signal is spread out over multiple pixels. Hence it is not sure that this effects the profile plots, since the average PA value over 3 columns would then be the same.

Another explanation could be that at the different depths a different light fluence reaches the tubes. Due to the usage of two linear laser arrays, which emit light under a certain angle, the light fluence initially increases in the medium, but at larger depths decays again. If this is the reason for the different profile plots, then the profile plot could possibly be used to provide information about the fluence at a particular depth. Further investigation will be necessary to verify this.

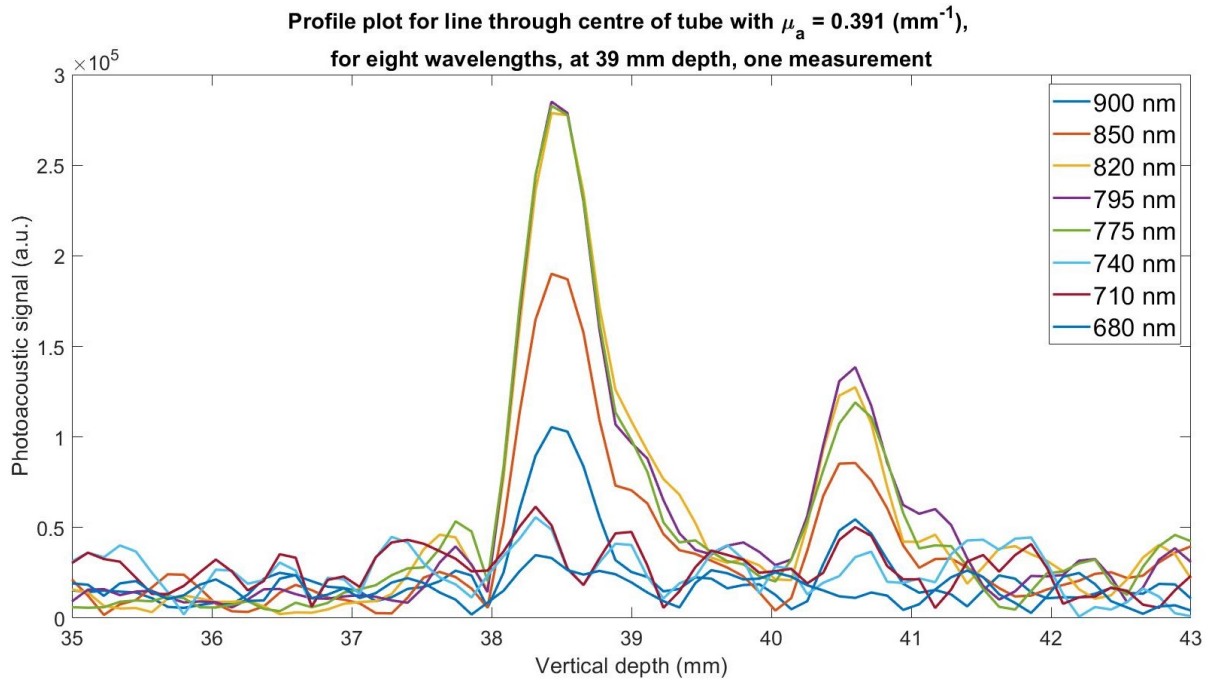


(a) Profile plot of PA value through middle of the tube with $\mu_a = 0.391 \text{ mm}^{-1}$ for 8 different wavelengths.

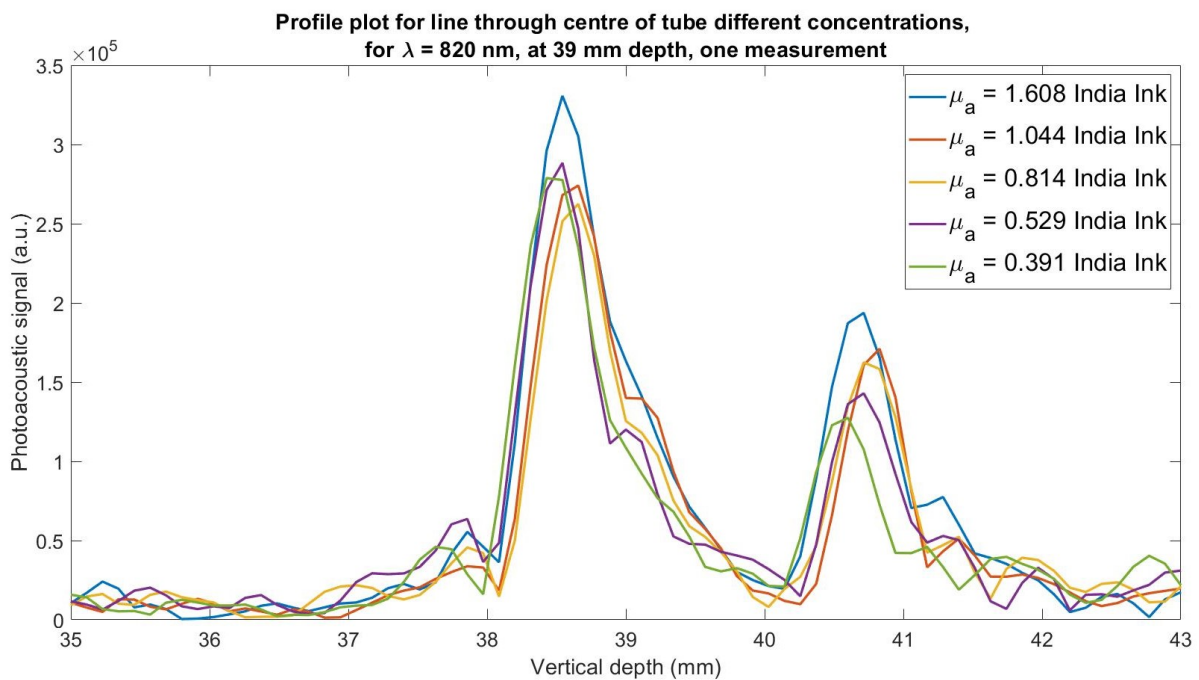


(b) Profile plot of PA value through middle of the tube with 5 different concentrations for $\lambda = 680 \text{ nm}$. The μ_a that are shown in the legend have the unit mm^{-1} and are the values corresponding to $\lambda = 800 \text{ nm}$

Figure 12: Different profile plots for India Ink solutions at 24 mm depth. PA values are not pulse energy compensated.



(a) Profile plot of PA value through middle of the tube with $\mu_a = 0.391 \text{ mm}^{-1}$ for 8 different wavelengths.



(b) Profile plot of PA value through middle of the tube with $\mu_a = 0.391 \text{ mm}^{-1}$ for 8 different wavelengths. The μ_a that are shown in the legend have the unit mm^{-1} and are the values corresponding to $\lambda = 800 \text{ nm}$

Figure 13: Different profile plots for India Ink solutions at 39 mm depth. PA values are not pulse energy compensated.

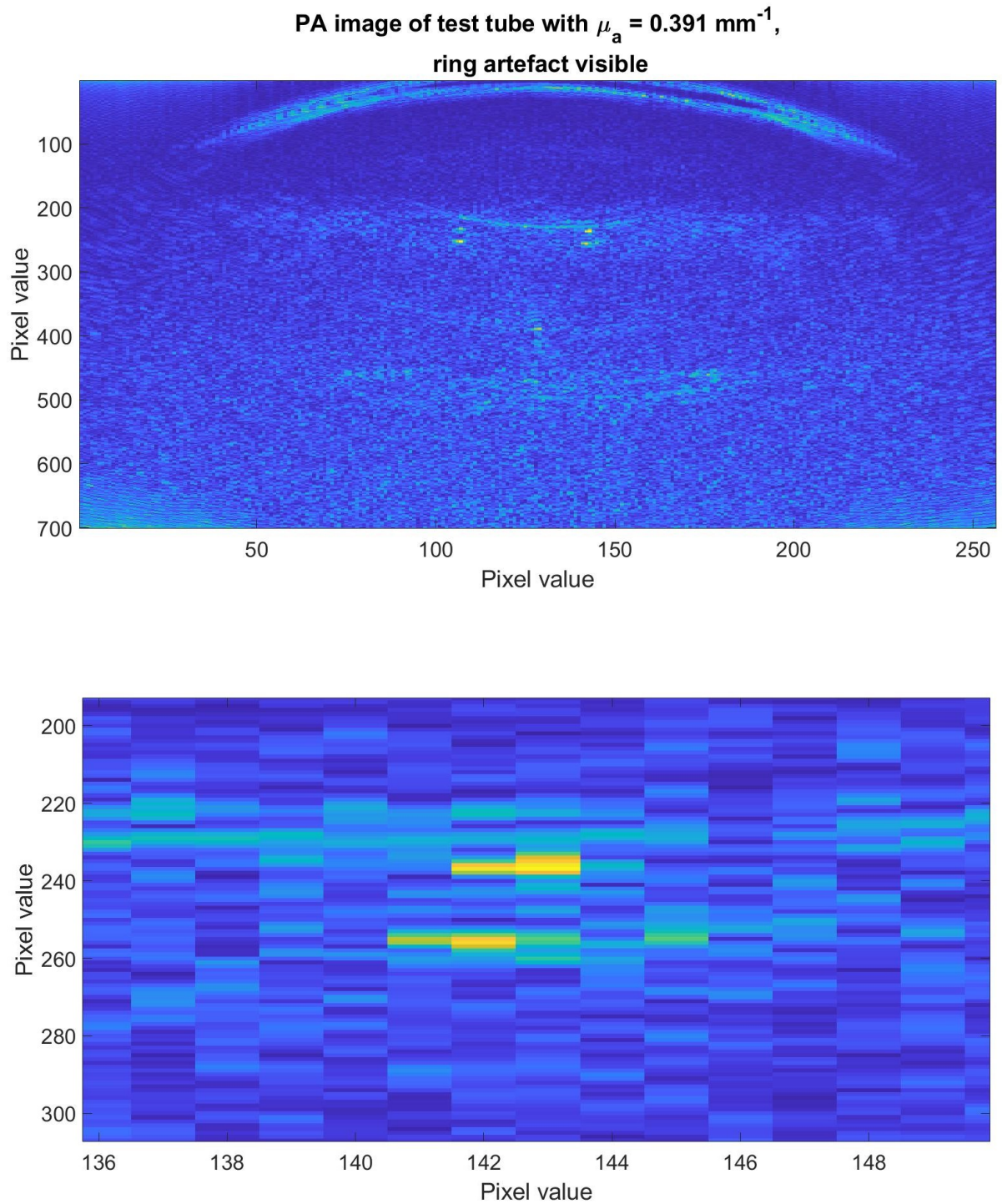
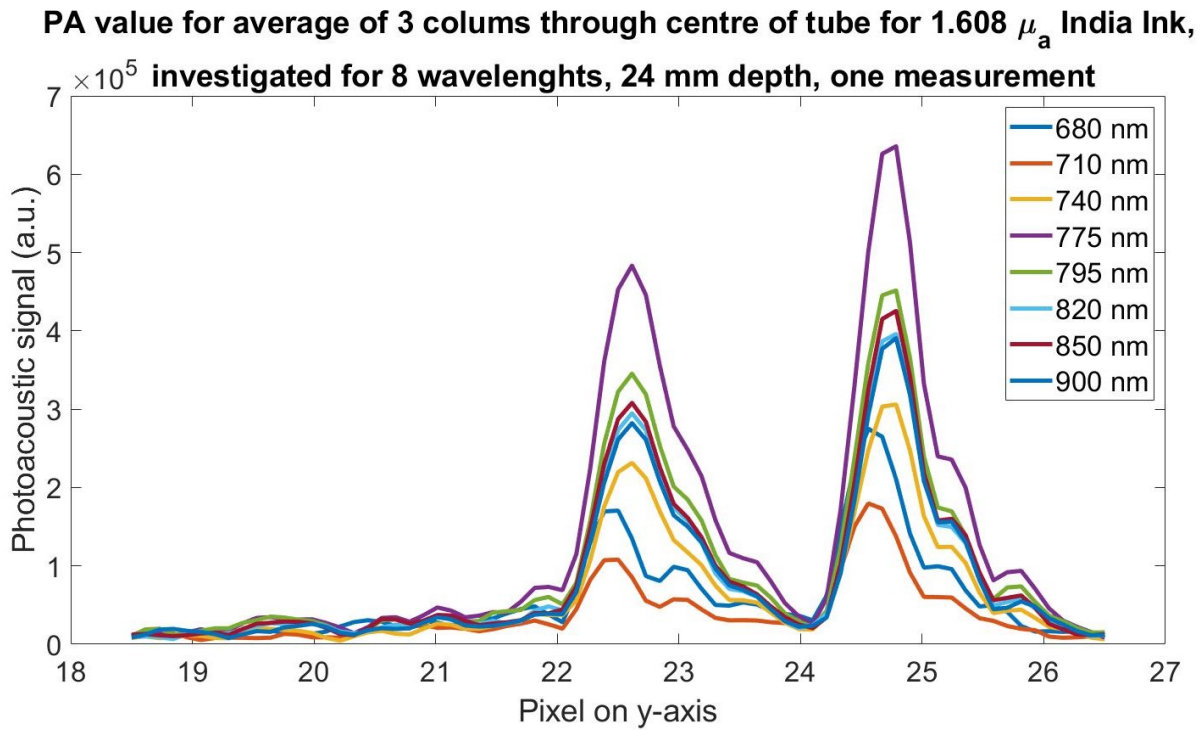
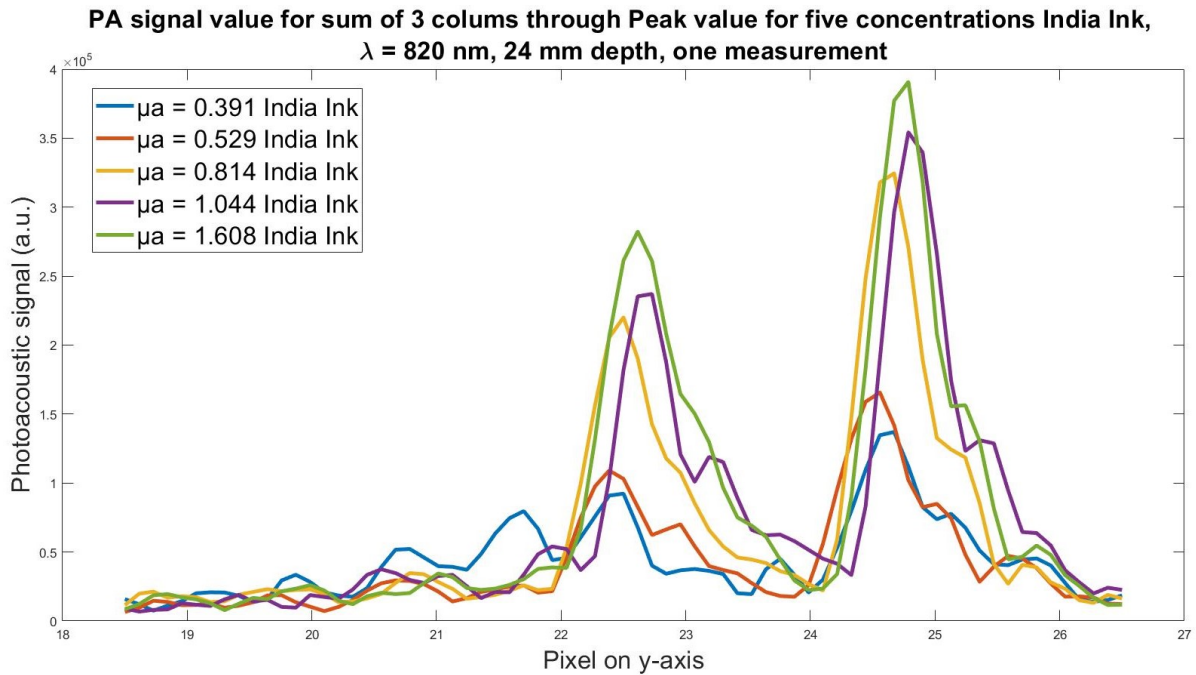


Figure 14: (a): A ring artefact is visible above the tube with two bands with a higher intensity; (b): PA image of the test tube with $\mu_a = 1.608 \text{ mm}^{-1}$, zoomed in on the tube to show difference lateral location of maximum in top and bottom region.

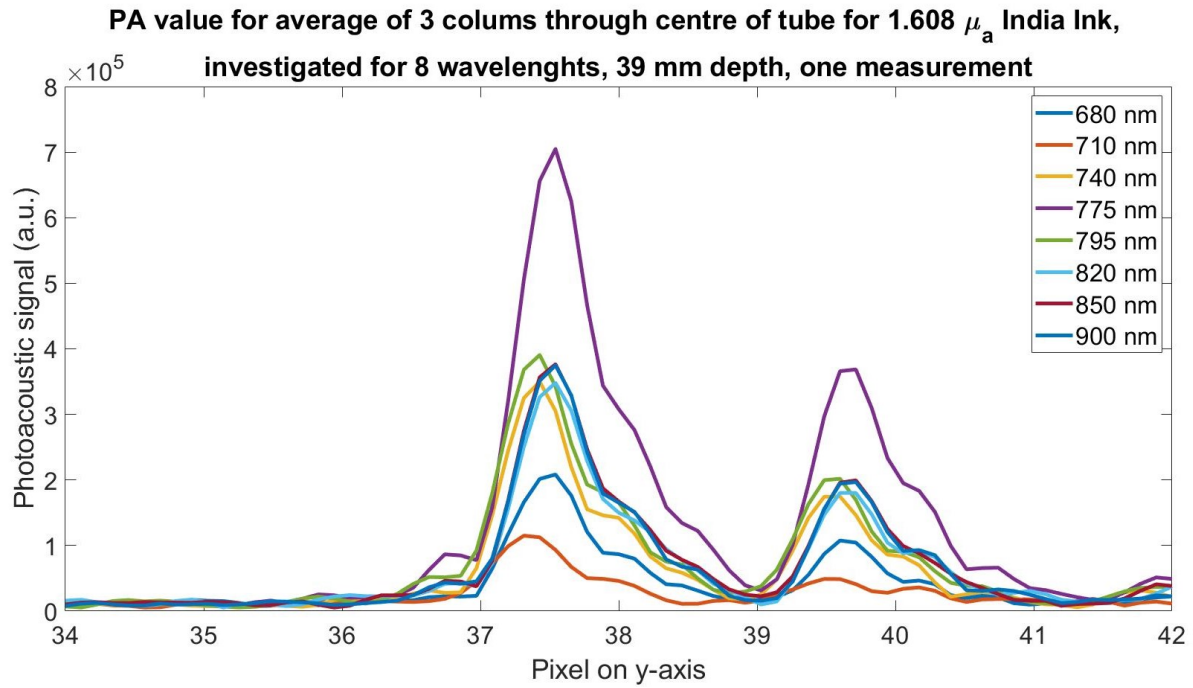


(a) Profile plot of average PA values over three columns through centre of the tube with $\mu_a = 0.391 \text{ mm}^{-1}$ for 8 different wavelengths.

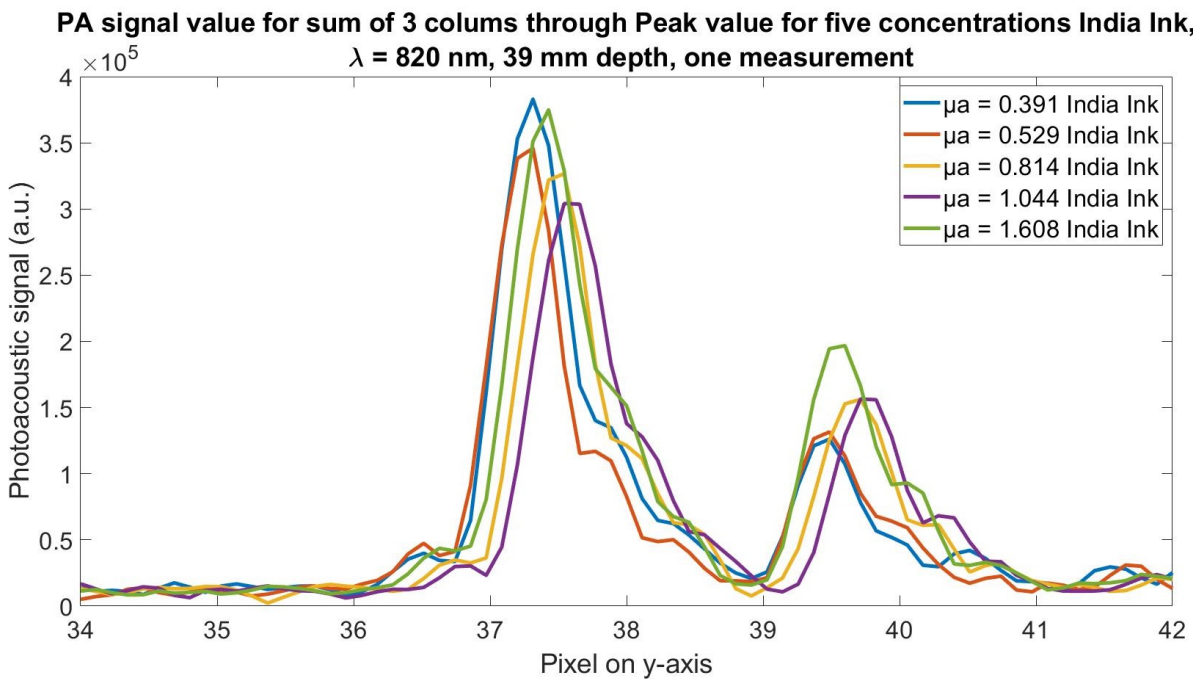


(b) Profile plot of average PA values over three columns through centre of the test tube with 5 different concentrations for $\lambda = 820 \text{ nm}$. The μ_a that are shown in the legend have the unit mm^{-1} and are the values corresponding to $\lambda = 800 \text{ nm}$

Figure 15: Different profile plots for India Ink solutions at 24 mm depth. PA values are not pulse energy compensated.



(a) Profile plot of average PA values over three columns through centre of the tube with $\mu_a = 0.391 \text{ mm}^{-1}$ for 8 different wavelengths.



(b) Profile plot of average PA values over three columns through centre of the test tube with 5 different concentrations for $\lambda = 820 \text{ nm}$. The μ_a that are shown in the legend have the unit mm^{-1} and are the values corresponding to $\lambda = 800 \text{ nm}$

Figure 16: Different profile plots for India Ink solutions at 24 mm depth. PA values are not pulse energy compensated.

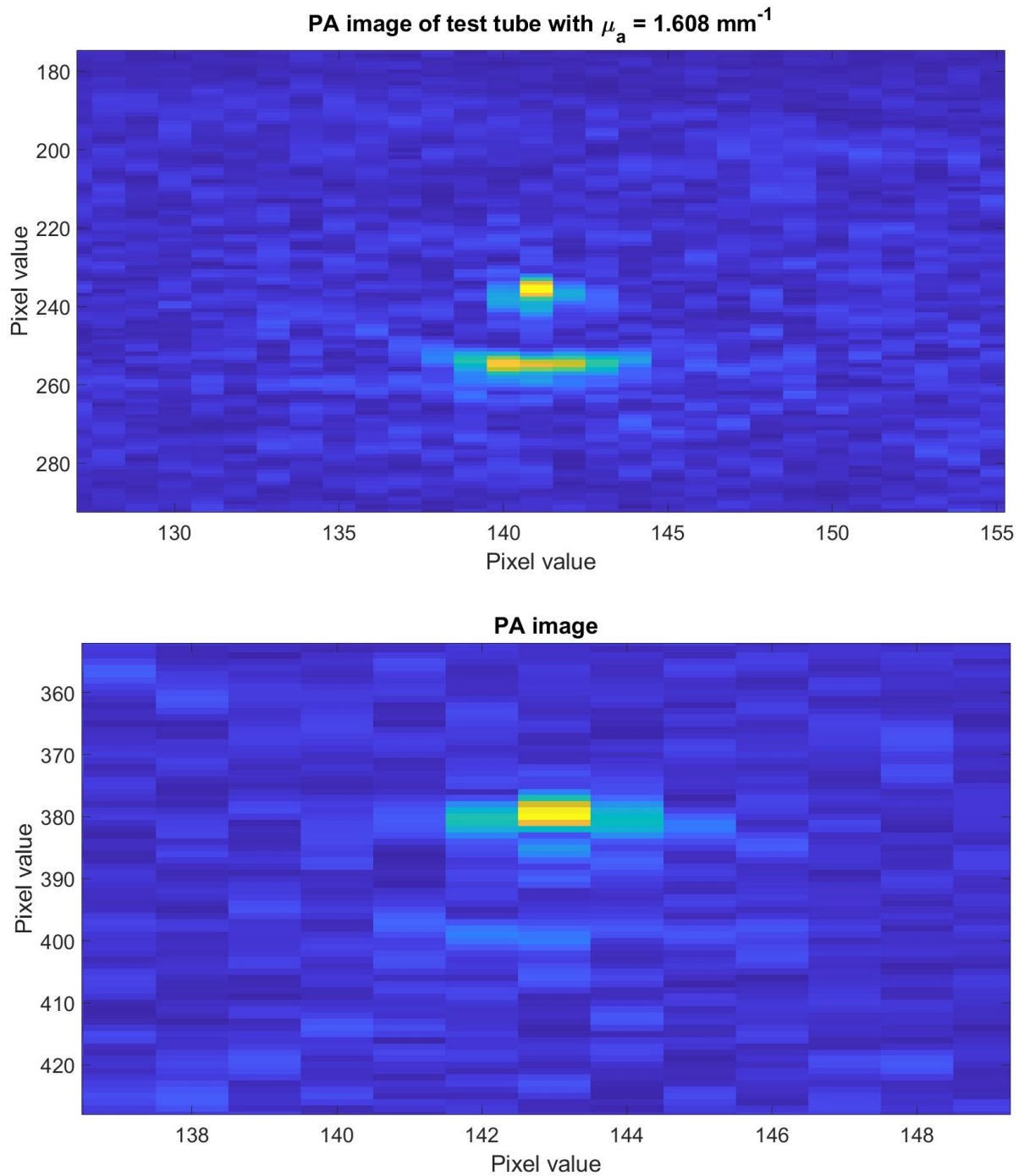


Figure 17: (a): PA image of the test tube located at 24 mm depth, where it is visible that the top part of the tube gives a narrower signal than the bottom part. (b): PA image of the test tube located at 39 mm depth, where the signal at the top of the tube is higher and broader than at the bottom part.

5.2 Pulse energy compensated

To find a possible explanation for the non expected shape of the spectrum of the photoacoustic signal versus wavelength, an analyse method was made to compensate the signal for the laser pulse energy. This was done, because it was expected that the laser light has different pulse energies for different wavelengths. The pulse energy of a laser beam is directly linked to the light fluence and therefore a change in pulse energy could declare the difference spectrum compared to the absorption spectrum.

To compensate for this pulse energy and therefore check if this is indeed the explanation for the outcome of the experiment, pulse energy is measured for every measurement. Like described in Paragraph 4.4, the pulse energy is measured before and after each measurement. This is done by flipping a mirror before the laser beam, directly behind the point where the laser light is emitted. The laser beam is then send onto a pulse energy meter, which displays the average pulse energy for every 3 seconds. The average pulse energy is calculated from those two values and then it is assumed that this was the pulse energy during the measurement. In Table 3, the pulse energies for one measurement with $\mu_a = 0.391$ for $\lambda = 800 \text{ nm}$ India Ink located at 24 mm depth are shown. In Appendix I all the measured pulse energies for all the different measurements are shown.

Wavelength (nm)	P before (mJ)	P after (mJ)	P average (mJ)
680	2.60	2.40	2.50
710	3.65	3.80	3.73
740	3.95	3.95	3.95
775	3.85	3.80	3.83
795	3.50	3.55	3.53
820	3.55	3.60	3.58
850	3.60	3.65	3.63
900	3.35	3.30	3.33

Table 3: Pulse energies for one measurement with $\mu_a = 0.391$ for $\lambda = 800 \text{ nm}$ India Ink located at 24 mm depth

Then, before calculating the average PA signal of the tube with India Ink, the whole signal is divided by this pulse energy. This is done for every measurement with the pulse energy that was measured during that specific measurement. In this way the signal is compensated for the pulse energy. After this is done, the average PA value is calculated in the same way as before. Those values are plotted against the corresponding wavelengths in Figure 18.

Reviewing these results, it can be noted that the amount of increase at the $\lambda = 710 \text{ nm}$ is decreased, but is still there. Before compensating the signal, the PA values at $\lambda = 710 \text{ nm}$ are almost twice as high as the values at $\lambda = 680 \text{ nm}$ and after compensating the increase is less than two times. The increase around $\lambda = 800 \text{ nm}$ is still there and did not change much compared to the signal before compensating. Regarding the relation between different concentrations, the linearity is still not visible. For the values at 24 mm depth, the values of the highest two concentrations are almost identical and the also the lowest two are really close to each other, with sometimes a higher signal for the lowest concentration than for the second lowest concentration. For the values at 39 mm depth, the increase at $\lambda = 710 \text{ nm}$ is not seen for the concentrations with $\mu_a = 0.391 \text{ mm}^{-1}$, $\mu_a = 0.814 \text{ mm}^{-1}$ and $\mu_a = 1.044 \text{ mm}^{-1}$ at $\lambda = 800 \text{ nm}$. Overall it seem that there is more dispersion of the PA values at 24 mm depth than at 39 mm depth, when looking at different concentrations. The error bars are a generally smaller for the PA values from 24 mm depth than at 39 mm depth at $\lambda = 680 \text{ nm}$ and $\lambda = 710 \text{ nm}$, meaning that different measurements of the same concentration India Ink gave average PA values of the ROI that are

closer to each other for a depth of 24 mm than for a depth of 39 mm.

Since the overall shape of the graph is still not similar to the absorption spectrum measured with the spectrophotometer, it is expected that there are more external variables which influence the measured PA signal. Another compensation method is desired which takes care of all these factors.

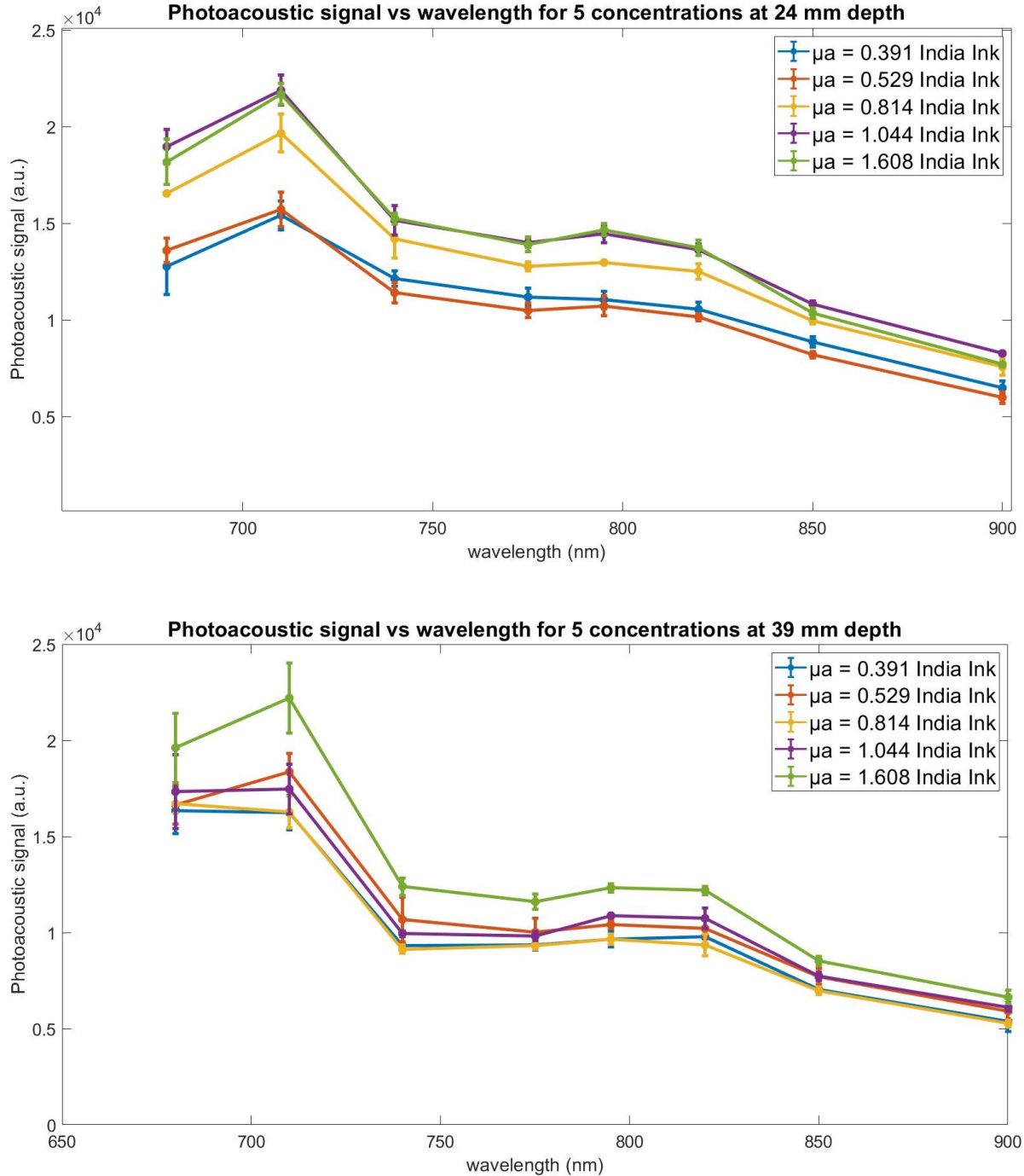


Figure 18: Average PA signal, of three measurements after compensating for the pulse energy in each measurement, versus wavelength for 5 different concentrations, with tubes located at 39 mm depth. The μ_a that are shown in the legends have the unit mm^{-1} and are the values corresponding to $\lambda = 800 \text{ nm}$

5.3 Compensating for difference in reference tube

As described in Paragraph 4.4, every photoacoustic measurement was done for two tubes simultaneously. The reference tube always contained a $\mu_a = 0.391 \text{ mm}^{-1}$ for $\lambda = 800 \text{ nm}$ solution of India Ink and the test tube had a varying concentration of India Ink for the different measurements. The tubes were located at the same depth, but were laterally 6 mm removed from each other.

Since the reference tube always contains the same concentration, ideally the PA signal should always be the same. When there is a difference in the reference tube, this must be due to external factors, including for instance the pulse energy difference like discussed before. In this analyse method, it is assumed that all the external factors that have an influence on the test tube also have the exact same influence on the reference tube. Then by comparing the differences in the signals from the reference tubes, it is possible to receive weight factors which can compensate for those difference. These weight factors are gained by shifting every average PA signal of the reference signal for one wavelength to the exact absorption coefficient value corresponding to that wavelength, which was measured with the spectrophotometer. Eq. 7 shows the formula which is used to calculate the weight factors. It takes the value of the actual absorption coefficient of the concentration present in the reference tube for one specific wavelength. Than it divides this value with the average PA value of the reference tube for that same wavelength. Eventually this is done for every wavelength and for every measurement, providing a large 6x40 matrix with weight factors which are each specific for one single measurement. Like discusses in Paragraph 4.4, every concentrations of India Ink at a specific depth is measured three times for every wavelength. On row 1 to 3, the weight factors are noted for these three different measurement with the tubes located at a depth of 24 mm. On row 4 to 6, the weight factors are noted for the tubes located at 39 mm depth.

The compensation is finally done by multiplying the weight factor coming from measurement x with the average PA value of the test tube from measurement x , as shown in Eq. 8. This is done for all the measurements. All the values that play a role in this compensations for one measurement with the tubes located at 39 mm depth are shown in Table 4. The *actual absorption coefficient* is the absorption coefficient measured with the spectrophotometer for the concentration of India Ink which is present in the reference tube.

$$W_\lambda = \mu_a(\lambda) / PA_{(ref, \lambda)} \quad (7)$$

$$PA_{(compensated, \lambda)} = PA_{(uncompensated, \lambda)} * W_\lambda \quad (8)$$

Wavelength (nm)	680	710	740	775	795	820	850	900
Actual absorption coefficient (mm^{-1})	0.48	0.46	0.44	0.41	0.40	0.39	0.37	0.35
Measured PA signal reference tube ($*10^4$)	2.61	3.88	2.50	2.29	2.15	2.12	1.59	1.27
Calculated weight factor ($*10^4$)	0.18	0.12	0.17	0.18	0.19	0.18	0.23	0.27
Uncompensated PA signal test tube ($*10^4$)	3.55	6.05	3.50	3.36	3.26	3.20	2.44	1.57
Compensated PA signal test tube	0.66	0.71	0.61	0.61	0.61	0.58	0.57	0.43

Table 4: Example of all the components with their values to receive the compensated PA signal of the test tube. Example for measurement 1 with the tubes at 39 mm depth.

5.3.1 Results for photoacoustic signal versus wavelength

In the Figures 19 and 20, the analyse method is visualised and in Figure 21 the final results of the compensated test tubes are shown.

Figure 19a shows the PA signal coming from the reference tube versus wavelength. The different lines reflect the reference tube located next to the a test tube with different India Ink solutions. As stated earlier, ideally the signal of the reference tube should always be the same, since the concentration is constant. As can be seen, there is a significant difference in all the PA values coming from all the different measurements.

The weight factors are determined by dividing the actual absorption coefficient by the measured PA value for a single wavelength and measurement. For example for $\lambda = 680nm$ holds $\mu_a = 0.48 mm^{-1}$, then five weight factors are determined, all by dividing $\mu_a = 0.48 mm^{-1}$ by the PA value for the reference tube at $\lambda = 680nm$. This is done for all the eight wavelengths.

In Figure 19b, all the five curves of Figure 19a are multiplied with the weight factors belonging to each data point. The result is five overlapping curves, which is as expected since all the curves are weighted to the same actual absorption coefficient. The curve shows a exponential decay, just as the absorption spectrum of India Ink does.

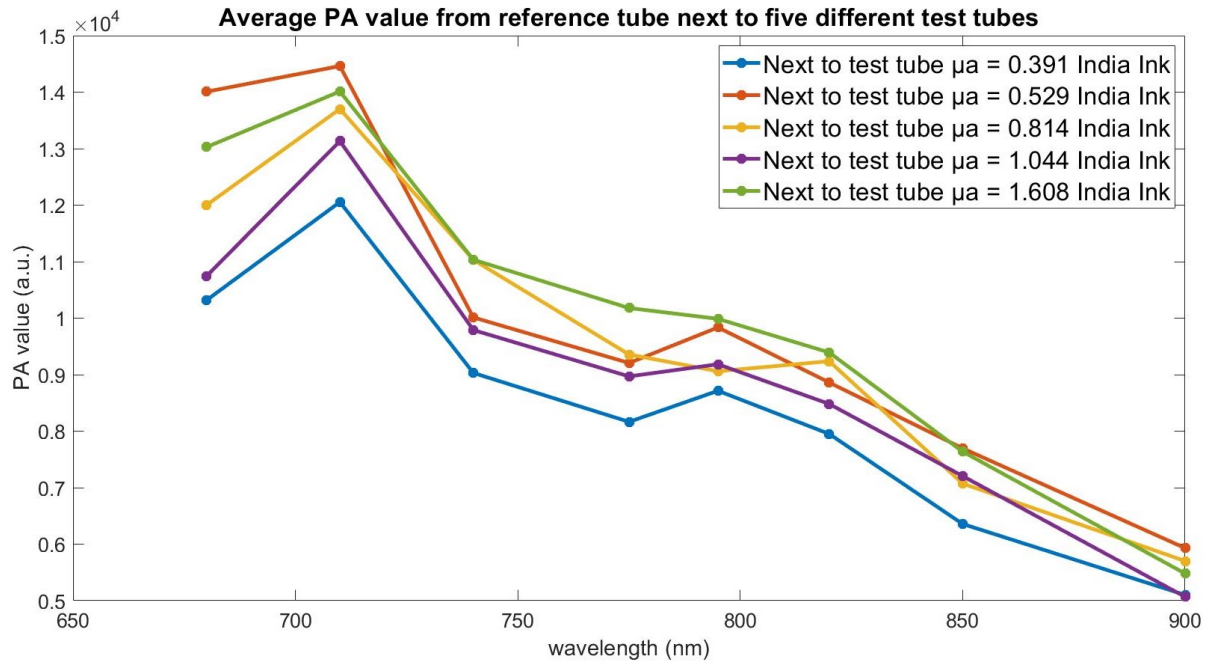
In Figure 20a the uncompensated PA signals versus wavelength are shown for the test tube. All the data points in this plot are multiplied with the same weight factors which were calculated before. The results for one measurement with tubes located at 24 mm depth are shown in Figure 20b. After compensating, the PA values are considered to be estimated μ_a values, since they are weighted with factors which bring the PA values coming from the reference tube to the actual absorption coefficient.

Eventually this compensation is done for all the different measurements, so three times for the tubes located at 24 mm depth and three times for the tubes located at 39 mm depth. The averages of these values for every wavelength and every concentration are plotted in Figure 21 with the standard deviation as error bars. With red dashed lines, exponential fits are plotted through the curves.

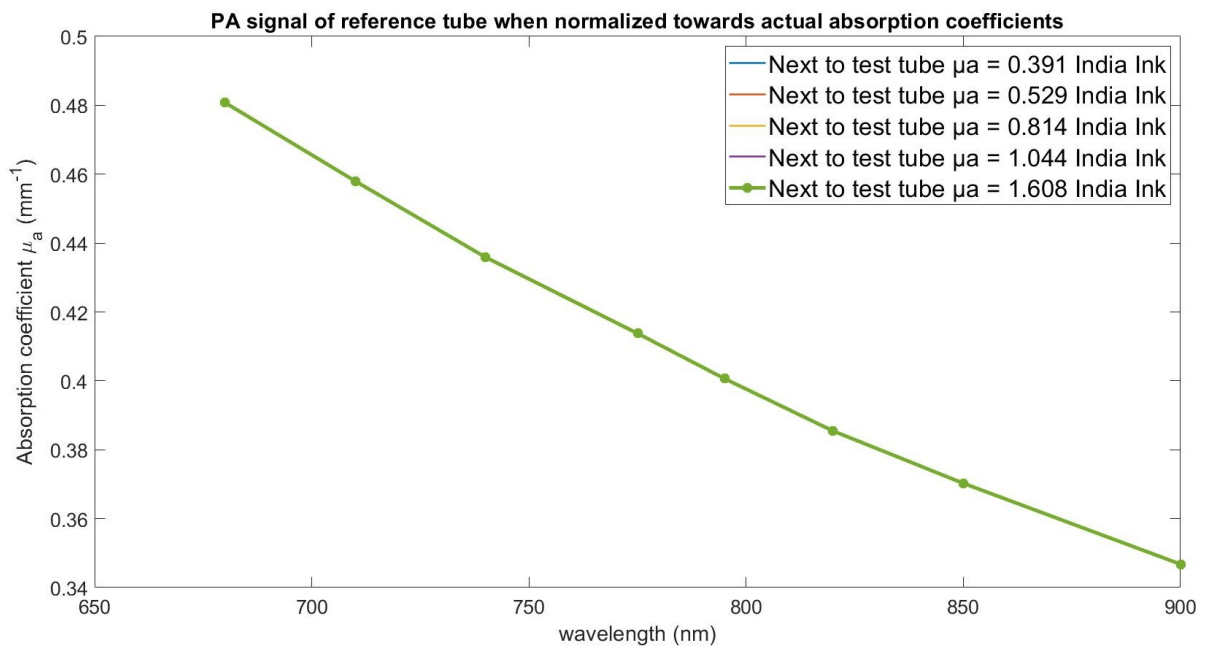
Overall, there is a decay visible of the estimated absorption coefficient with wavelength. There is still an increase visible at $\lambda = 710 nm$, but this is much smaller than at the beginning. The increase around $\lambda = 800 nm$ is more smoothed out.

The different concentrations do not show linearity with the estimated μ_a . For the tubes located at 24 mm depth, the estimated μ_a have values further apart from each other, which makes it easier to distinguish the different curves in the plot. the estimated μ_a follows the order of concentrations: the lower concentrations give lower estimated μ_a values and the higher concentrations give higher estimated μ_a values. The only exception here is that for the lowest concentration the estimated μ_a value is higher than the estimated μ_a for the second lowest concentration for the wavelengths $\lambda = 850nm$ and $\lambda = 900nm$.

For the tubes located at 39 mm depth, the estimated μ_a values are less separated from each other. The three highest concentrations have approximately the same estimated μ_a values as for the tubes at 24 mm depth, but the two lowest concentrations have higher values at 39 mm depth than at 24 mm depth. The curve corresponding to $\mu_a = 0.814 mm^{-1}$ India Ink shows fluctuating behaviour, but also has relatively large error bars.

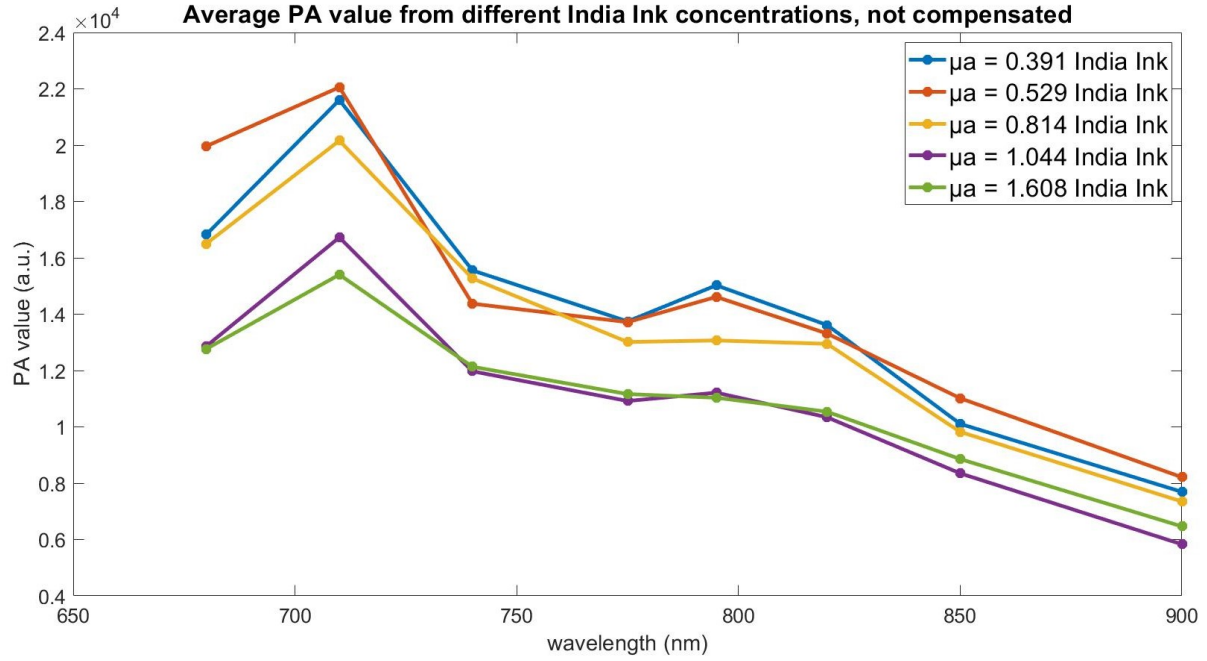


(a) PA value of reference tube, not compensated.

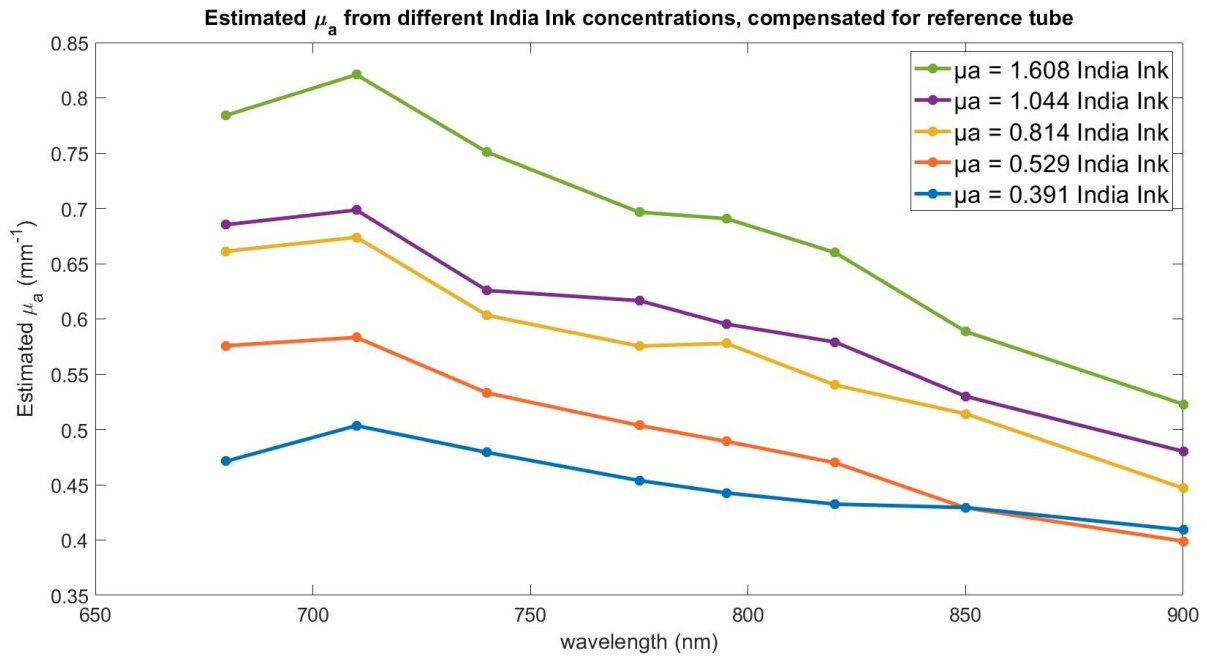


(b) Average PA value of reference tube forced to correct absorption spectrum

Figure 19: PA value of the reference tube ($\mu_a = 0.391 \text{ mm}^{-1}$ for $\lambda = 800 \text{ nm}$) without compensation (top) and after it is forced to the absorption spectrum of India Ink $\mu_a = 0.391 \text{ mm}^{-1}$ for $\lambda = 800 \text{ nm}$ (bottom). Both with tubes located at 24 mm depth. The μ_a that are shown in the legend have the unit mm^{-1} and are the values corresponding to $\lambda = 800 \text{ nm}$

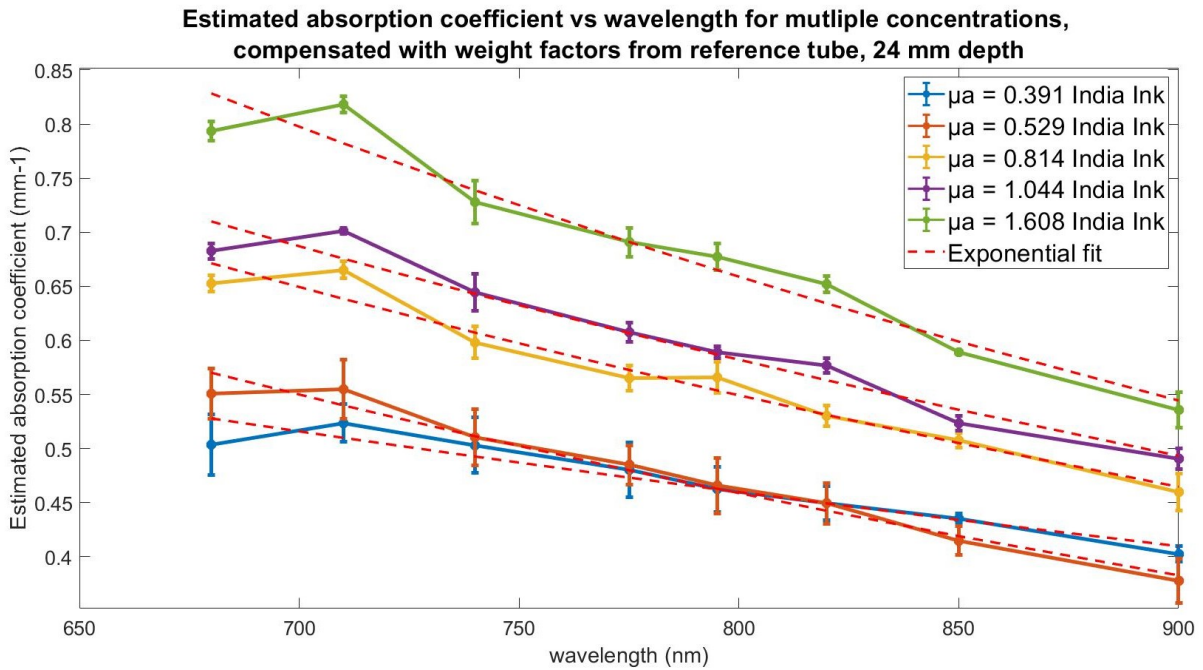


(a) PA value of test tube, not compensated.

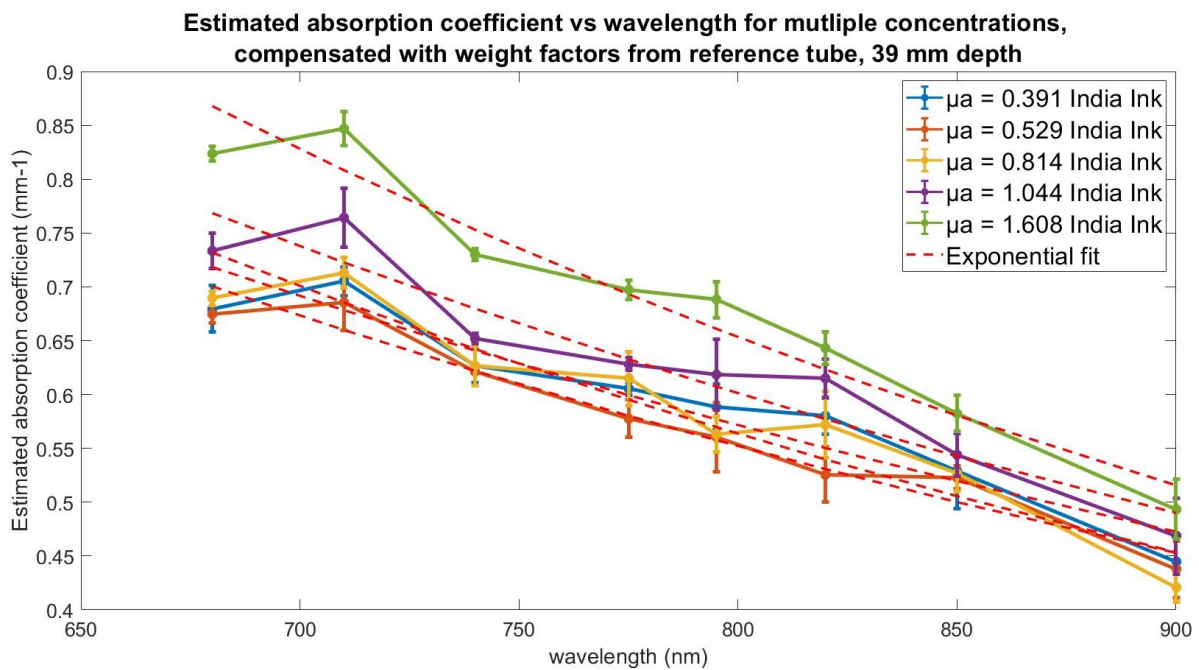


(b) PA value of test tube compensated with weight factors from reference tube.

Figure 20: PA values of the test tube with 5 different concentrations India Ink without compensation (top) and the estimated μ_a after compensating for the reference tube (bottom). Both with tubes located at 24 mm depth. The μ_a that are shown in the legend have the unit mm^{-1} and are the values corresponding to $\lambda = 800 \text{ nm}$



(a) Average estimated μ_a of three measurements for 5 concentrations India Ink and 8 wavelengths. Tubes located at 24 mm depth.



(b) Average estimated μ_a of three measurements for 5 concentrations India Ink and 8 wavelengths. Tubes located at 39 mm depth. spectrum

Figure 21: Average estimated μ_a for two different depths. PA values are compensated with weight factors coming from the reference tube to get estimated μ_a values. Exponential fit is plotted as red dashed lines. The μ_a that are shown in the legend have the unit mm^{-1} and are the values corresponding to $\lambda = 800 \text{ nm}$

5.3.2 Actual versus estimated μ_a values

As discussed before, the reference tube is weighted to the actual absorption coefficients of its concentration India Ink. Because the weight factors are determined for every measurement, it is assumed that those weight factors will compensate for all the different external variables. Therefore, in the ideal situation, the estimated and actual μ_a values should have the same value when the test tube is compensated with the same weight factors. When the actual μ_a is plotted against the estimated μ_a , a linear line with a slope of 1 is expected. Furthermore, when different concentrations of India Ink solutions are investigated for multiple wavelengths, the analysis should ideally give the same estimated μ_a values if the actual μ_a has the same value. So for example, if solution 1 has an actual μ_a value of 0.5 mm^{-1} for $\lambda = 680 \text{ nm}$ and solution 2 has also an actual μ_a value of 0.5 mm^{-1} , but than for $\lambda = 820 \text{ nm}$, than the estimated μ_a values should be the same when the solutions are analysed for $\lambda = 680 \text{ nm}$ and $\lambda = 820 \text{ nm}$, respectively.

In Figure 22 the plots are shown in which the actual μ_a is plotted against the estimated μ_a as a scatterplot. The estimated μ_a is the mean value of the three measurements. In the Figure, also a linear fit is plotted for which the function is shown in the legend.

It can be noted that the expectations of the ideal situations are not met. The estimated absorption coefficients are not the same as the actual absorption coefficients for both when the tubes are located at 24 mm as 39 mm depth. The relation between actual and estimated μ_a seems to be linear, but not proportional. Every concentration gives rise to a linear fit with a different slope. For both depths, the slopes of the fitted lines are decreasing over concentration, only the linear fit for $\mu_a = 0.529 \text{ mm}^{-1}$ is an exception on this rule, since this concentration shows an increase compared to the slope of the linear fit from the lowest concentration. For the slopes of the tubes located at 24 mm depth, the slope of the lowest concentration has a value around 0.87, as can be seen in the legend of subfigure (a). Then, there is a decrease visible, which has an exponential character, to give eventually a slope for the highest concentration with a value around 0.52. For the tubes located at 39 mm depth, the slope for the lowest concentration has a value of 1.82 and for the highest concentration a value around 0.64. Also here the decrease of slope over concentration has an exponential decaying character.

The other expectation that the etimated μ_a value should be the same if the actual μ_a value is the same, is not the seen in the results. For instance the estimated μ_a values of the linear fit for $\mu_a = 0.391 \text{ mm}^{-1}$ are higher than those of the the linear fit for $\mu_a = 0.529 \text{ mm}^{-1}$, when the actual μ_a values are the same.

At this point it is not sure what is causing the fact that there is not a proportional linear relation seen between the PA signal and the concentration. The stiffness of the tube might have an influence. Simply expressed, if the tube has a high stiffness, the expansion of the ink particles is resisted by the wall of the tube. Therefore the ink could possibly have less capability of generating a US wave. Furthermore, it is expected that the acoustic attenuation in the tube is different for different frequencies. Here is it expected that higher concentrations of India Ink will produce high-frequency signals from the boundary of the tube.

5.3.3 Concentration versus estimated μ_a values.

Now it is also possible to plot the concentration of the solutions versus the estimated μ_a values. These plots are shown in Figure 23. The concentrations of India Ink are shown on the x-axis. Every concentration is measured for eight different wavelengths, so for the concentration of $\mu_a = 0.391 \text{ mm}^{-1}$ at $\lambda = 800 \text{ nm}$ eight different estimated μ_a values are plotted. The calculated estimated μ_a values, coming out of the data analysis, are shown as scatter plots. The corresponding lines are exponential fitted curves through the data points belonging to one specific wavelength. There has been chosen an exponential fit because the scatter plots showed exponential behaviour. Note that both the curve for $\lambda = 680 \text{ nm}$ as for $\lambda = 900 \text{ nm}$ are coloured

red. There are also eight other curves plotted, which correspond to the actual μ_a values over concentration for different wavelengths. Those are the curves with a bigger slope and higher end value in the plots. For these curves, it holds that the top curve belongs to the values corresponding to $\lambda = 680 \text{ nm}$ and that the bottom curve belongs to the values corresponding to $\lambda = 900 \text{ nm}$.

For both depths, the curves with the lowest concentrations give the highest estimated μ_a values, which corresponds to the absorption spectrum of India Ink. This results is also not surprising since it is in line with the results showed in Figure 21. The estimated μ_a value increases with the concentration of India Ink, which is also as expected, but it does not seem to have the same relation as the actual μ_a does. The actual μ_a shows a linear relation between the concentration and the absorption coefficient, while this looks more like an exponential relation for the estimated μ_a and concentration. As discussed in Paragraph 3.2 and showed in Figure 3, there are cases in which the relation between PA signal and the μ_a is not proportional linear. As can be seen in Figure 3, the curve is first linear and then becomes exponential with a decreasing slope over concentration. In Figure 23 the slope seems to be increasing instead of decreasing.

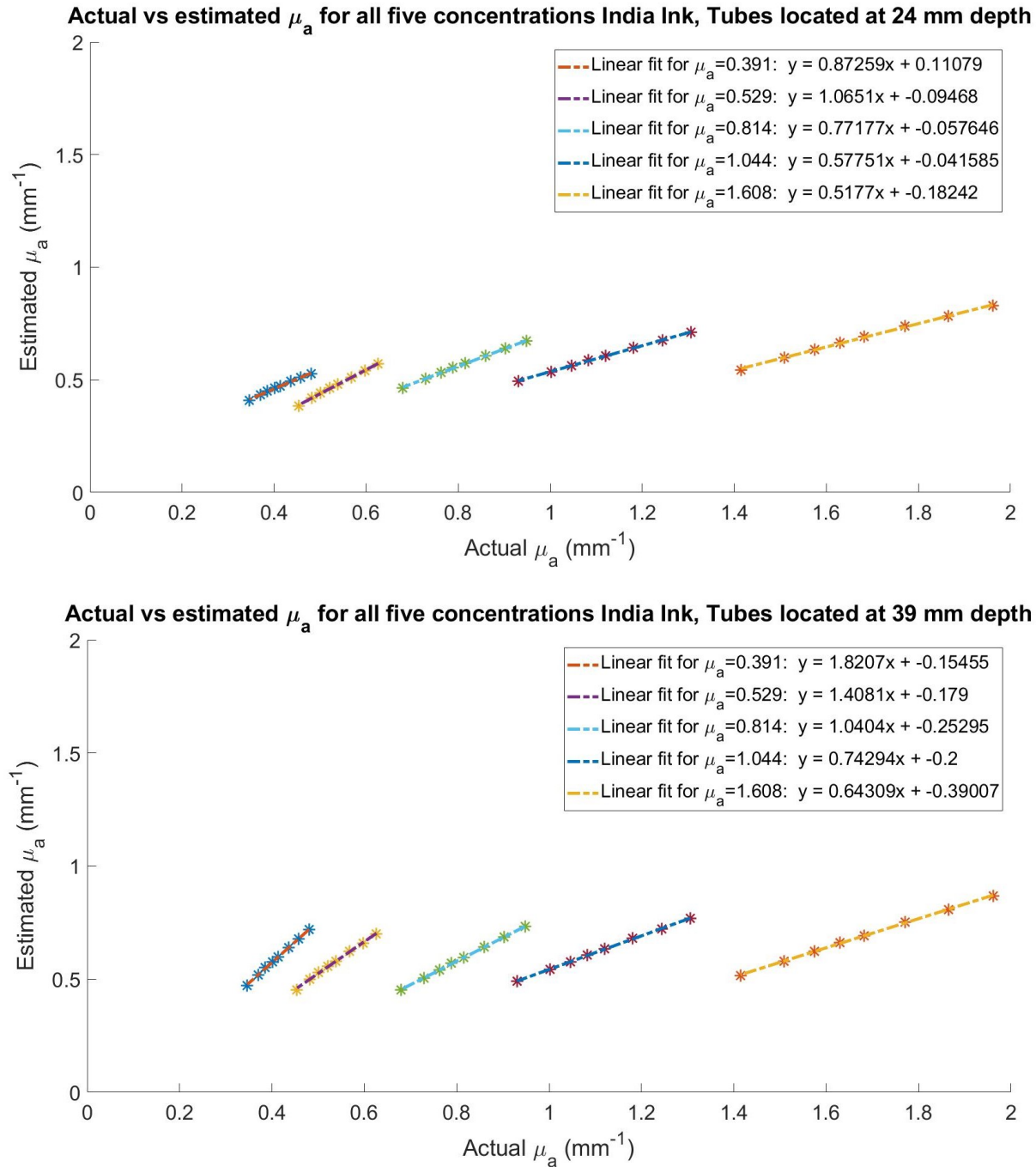


Figure 22: Estimated μ_a vs actual μ_a for five different concentrations of India Ink solutions. Top: tubes located at 24 mm depth; bottom: tubes located at 39 mm depth. The μ_a that are shown in the legend have the unit mm^{-1} and are the values corresponding to $\lambda = 800 \text{ nm}$

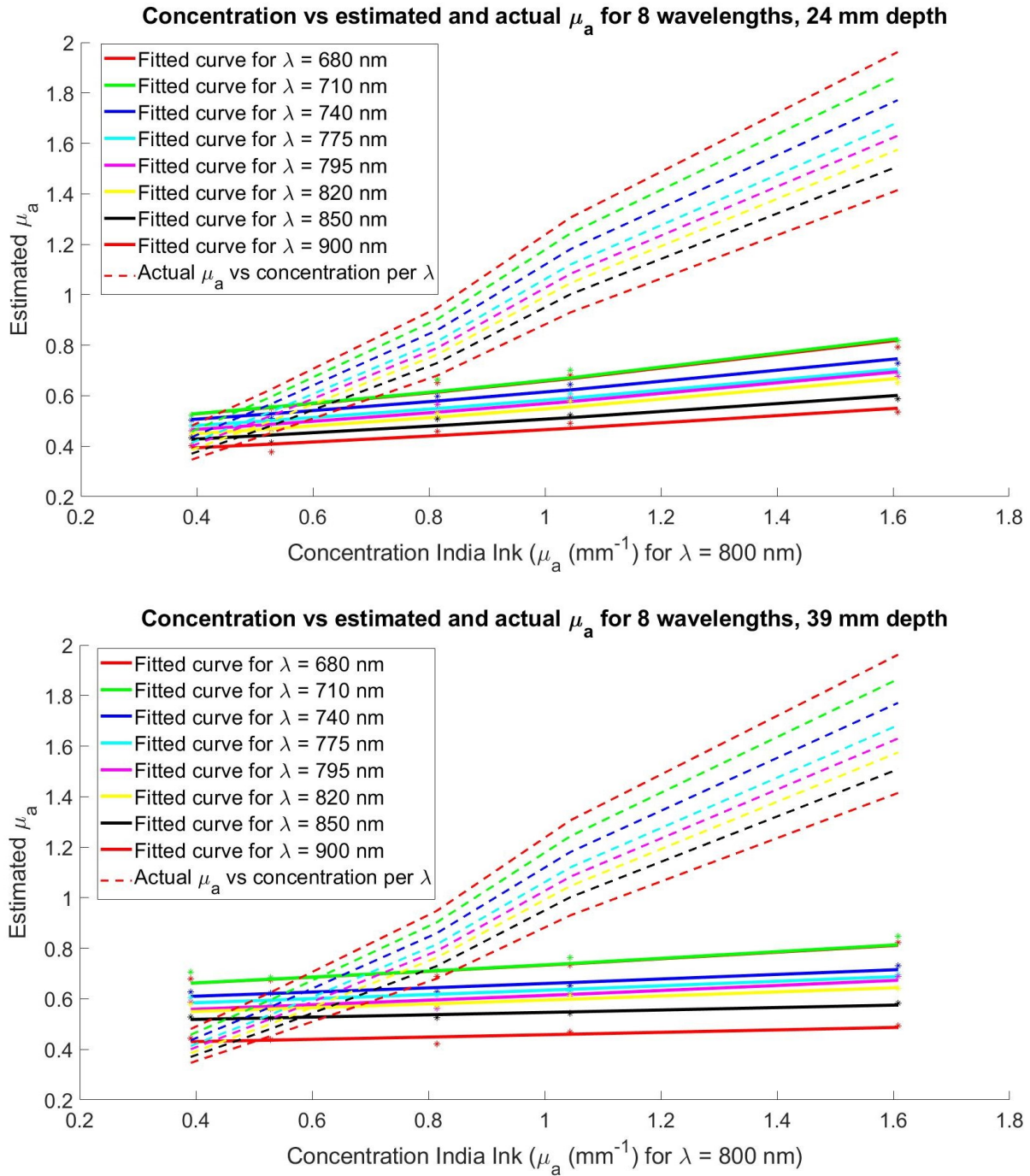


Figure 23: Concentration of India Ink solution vs the estimated μ_a values for eight wavelengths. The calculated estimated μ_a values are scattered, a exponential fitted line is shown. Also the actual μ_a versus concentrations are plotted, these are the curves with higher values and bigger slopes. The top curve corresponds to the highest concentration and the lowest curve to the lowest concentration. Top: Tubes located at 24 mm depth; bottom: Tubes located at 39 mm depth.

6 Conclusions and recommendations

It can be concluded that there are multiple external factors which influence the photoacoustic signal that is obtained using the experimental set up of this research. This results in spectra which do not directly correspond to the absorption spectra of the investigated substance, in this case India Ink. And furthermore, the relation between the PA signal and the concentration of the substance is not proportional linear.

Two compensation methods have been investigated, one compensating only for the pulse energy and one compensating for the differences in PA signal measured at the reference tube. The compensation for only the pulse energy brings the results more to the expected signal, but still has different spectra and non linearity in the signal. From this it can be concluded that the pulse energy does effect the PA signal but that it is not the only external factor.

When the PA signal is compensated for the differences measured at the reference tube, it was expected that all the external factors were taken into account. When looking at the results, the spectra became indeed much closer to the expected absorption spectra and there is a difference visible between the different concentrations of India Ink. Hence the conclusion can be made that the use of a reference sample is a good way to analyse an unknown sample. The compensation with respect to the reference tube is a good way to compensate for the external factors which are also effecting the test tube. In this study the reference and test tube contained the same chromophore, but it is expected that this method will also be useful when investigating a test tube with a different, unknown chromophore. However, the footnote should be made that the resulting spectrum obtained after the compensation method is still not exactly the same as the measured absorption spectrum from the spectrophotometer and that there is no proportional linearity between the absorption coefficient and the PA signal. To do a proper quantification analysis of an unknown chromophore, this linearity should be further studied. According the theoretical background, the experiment was done under such circumstances that the relation between the absorption coefficient and the PA signal should be linear. Recommended is to investigate why this is not seen in the results. A suggestion is to do the same experiment with a tube with a smaller diameter, because than there will be less fluence differences over the depth within the tube. It will have to be checked if the PA signal which is generated is high enough to be measured, since the background noise gives also quite a high signal. It is also recommended to do the same experiment with different types of tube which have a different stiffness. In this way it can be determined if the stiffness of the tube has an influences on the ultrasound wave that is produced and therefore has an influence on the PA signal that is measured.

When looking at the profile plots of the cross sections of the tubes, it is difficult to make solid conclusions. If the profile plots are made for one column through the centre of tube, the signal might not be representative for the true signal, since the lateral position of the maximum signal showed to be different for the top and bottom part in the tube for some measurements. When the average value is taken for three columns, it turns out that for the tubes located at 24 mm depth, the bottom part of the tube has a broader signal than the top part, while for the tube located at 39 mm depth this is not the case. There might be multiple explanations for this results. One being the characteristic of India Ink that ink particles settle down over time. This explanation is estimated unlikely, since the measurement for the tubes located at 24 mm depth took the same time as the measurements with the tubes located at 39 mm depth. The other explanation might be the use of a wrong speed of sound value in the reconstruction process. If the used speed of sound is too high, the bottom part of the tube might give a broader signal than the top part of the tube. However, a wrong value for the speed of sound gives indeed a wrong distribution of the PA signal in the reconstruction, but the total value of the signal should be equal. In other words, the average value over three columns should be similar for the top and bottom part. Hence it is not sure that this effects the profile plots. Further investigation is recommended, in which other speed of sounds should be applied.

A last explanation for this difference in profile plots might be a varying light fluence reaching the tubes at different depths. When this is the case, the profile plot could be possibly used as a indicator for the fluence at that particular depth. Further investigation is necessary, where tubes are measured at a larger variety of depths. Here it is important that it is ensured that settling down of ink can not take place and that the correct speed of sound is applied in the reconstruction.

7 Outlook

Concluding this study, it can be stated that there still has to be done research before quantitative photoacoustic imaging can be used to truly quantify an unknown chromophore, such as lipids, within the carotid artery. However, this research has promising results. The PA signals can be compensated such that they follow the line of the absorption spectrum and furthermore, a positive relation is seen between the PA signal and the different concentrations of the chromophore, even though it is not a proportional linear relation at the moment.

References

- (1) Medicine, J. H. Carotid artery disease. https://www.hopkinsmedicine.org/heart_vascular_institute/vascular-surgery/our-specialties/carotid-artery-disease.html (**urlseen** 15/06/2022).
- (2) Organization, W. H. The top 10 death causes. <https://www.who.int/news-room/fact-sheets/detail/the-top-10-causes-of-death#:~:text=The%5C%20top%5C%20global%5C%20causes%5C%20of,birth%5C%20asphyxia%5C%20and%5C%20birth%5C%20trauma%5C%2C> (**urlseen** 02/06/2022).
- (3) Nighoghossian, N.; Derex, L.; Douek, P. *Stroke* **2005**, *36*, 2764–2772.
- (4) Köstli, K. P.; Frenz, M.; Bebie, H.; Weber, H. P. *Physics in Medicine & Biology* **2001**, *46*, 1863.
- (5) Beard, P. *Interface focus* **2011**, *1*, 602–631.
- (6) Cox, B. T.; Laufer, J. G.; Beard, P. C.; Arridge, S. R. *Journal of biomedical optics* **2012**, *17*, 061202.
- (7) Sivaramakrishnan, M.; Maslov, K.; Zhang, H. F.; Stoica, G.; Wang, L. V. *Physics in Medicine & Biology* **2007**, *52*, 1349.
- (8) Bosschaart, N.; Edelman, G. J.; Aalders, M. C.; van Leeuwen, T. G.; Faber, D. J. *Lasers in medical science* **2014**, *29*, 453–479.

Appendix II. IMA_C5_3_PA_standAlone_avg MATLAB script.

```

1  %% File name IMA_C5_3_PA_standAlone PA acquisition only, Verasonics is triggered by Func.
   Gen. synchronous to flashlamp, then triggers q-switch
2  clear all
3  close all
4  % Specify system parameters
5  Resource.Parameters.numTransmit = 256; % no. of transmit channels, check if we can really
   do all at once
6  Resource.Parameters.numRcvChannels = 256; % no. of receive channels, check if we can
   really do all at once
7  Resource.Parameters.connector = 0; %tell system to use both 128-element connectors for
   256 element probe
8  Resource.Parameters.speedOfSound = 1485; % speed of sound in m/sec
9  Resource.Parameters.simulateMode = 0; % if = 1 runs in simulate mode
10
11 numAvg = 2; %number of averages to take
12
13 % Specify Trans structure array.
14 Trans.name = 'IMA_C5-3';
15 Trans.units = 'mm';
16 Trans.numelements = 256;
17 Trans = computeTrans(Trans);
18
19 % Specify Resource buffers.
20 Resource.RcvBuffer(1).datatype = 'int16';
21 Resource.RcvBuffer(1).rowsPerFrame = 1024; % allows for max depth of 256 wls
22 Resource.RcvBuffer(1).colsPerFrame = 256;
23 Resource.RcvBuffer(1).numFrames = numAvg; % minimum size is 1 frame.
24
25 % Prepare display window for reconstructed image
26 Resource.DisplayWindow(1).Type = 'Matlab'; %uses Matlab figure, works better with non-
   verasonics reconstruction
27 Resource.DisplayWindow(1).Title = 'IMA_C5-3 PAI';
28 Resource.DisplayWindow(1).pdelta = 0.3;
29 Resource.DisplayWindow(1).Position = [250,150, ... % lower lft corner pos.
   ceil(256*Trans.spacing/Resource.DisplayWindow(1).pdelta), ...
   ceil(512*0.5/Resource.DisplayWindow(1).pdelta)];
30
31 Resource.DisplayWindow(1).ReferencePt = [-127.5*Trans.spacing,0,0];
32 Resource.DisplayWindow(1).AxesUnits = 'mm';
33 Resource.DisplayWindow(1).Colormap = hot(256);
34 Resource.DisplayWindow(1).numFrames = 1;
35
36
37 % Specify Transmit waveform structure - throws an error if not given, not
38 % used for PA
39 TW(1).type = 'parametric';
40 TW(1).Parameters = [5.0,1.0,10,1]; % 5 MHz, square wave, 10 half-cycles, initially
   positive
41
42 % Specify TX structure array - throws an error if not given, not
43 % used for PA
44 TX = struct([]);
45 TX(1).waveform = 1; % use 1st TW structure.
46 TX(1).focus = 0;
47 TX(1).Apod = zeros(1,Trans.numelements);
48 TX(1).Steer = [0,0];
49 TX(1).Delay = computeTXDelays(TX(1));
50
51 %Specify TGC waveform structure
52 TGC(1).CntrlPts = [500,590,650,710,770,830,890,950];
53 TGC(1).rangeMax = 300;
54 TGC(1).Waveform = computeTGCWaveform(TGC);
55
56 % Specify Receive structure array - currently not working for a single
57 % average (i.e. no averaging)
58 Receive = struct([]);
59 n = 0;
60 for j = 1:Resource.RcvBuffer(1).numFrames
61     n = n+1;
62     Receive(n).Apod = ones(1, 256);
63     Receive(n).startDepth = 0;
64     Receive(n).endDepth = 128;
65     Receive(n).TGC = 1;

```

```

66     Receive(n).mode = 0;
67     Receive(n).bufnum = 1;
68     Receive(n).framenum = j;
69     Receive(n).acqNum = 1;
70     Receive(n).sampleMode = 'NS200BW'; % If BW of probe turns out to be nearer 55% than
        100%, maybe use BS100BW to save time
71     if numAvg > 1
72         n = n+1;
73         Receive(n).Apod = ones(1, 256);
74         Receive(n).startDepth = 0;
75         Receive(n).endDepth = 128;
76         Receive(n).TGC = 1;
77         Receive(n).mode = 1;
78         Receive(n).bufnum = 1;
79         Receive(n).framenum = j;
80         Receive(n).acqNum = 1;
81         Receive(n).sampleMode = 'NS200BW';
82     end
83 end
84
85 Process(1).classname = 'External';
86 Process(1).method = 'rekon_OA_freqdom_LEGION';
87 Process(1).Parameters = {'srcbuffer', 'receive', 'srcbufnum', 1, 'srcframenum', -1, 'dstbuffer',
        'none'};
88 Process(2).classname = 'External';
89 Process(2).method = 'PA_Reconstruct_DNS_LEGION';
90 Process(2).Parameters = {'srcbuffer', 'receive', 'srcbufnum', 1, 'srcframenum', -1, 'dstbuffer',
        'none'};
91
92 % Specify sequence events.
93 Event = struct([]);
94 trigDelay = 180;%trigger delay in s
95 SeqControl(1).command = 'triggerIn';
96 SeqControl(1).condition = 'Trigger_1.Rising';
97 SeqControl(1).argument = 1;
98 SeqControl(2).command = 'timeToNextAcq';
99 SeqControl(2).argument = 10000;
100 SeqControl(3).command = 'jump';
101 SeqControl(3).argument = 1;
102 SeqControl(4).command = 'returnToMatlab';
103 SeqControl(5).command = 'noop';
104 SeqControl(5).argument = trigDelay*5;
105
106 SeqControl(6).command = 'triggerOut';
107 SeqControl(6).condition = 'syncNone';
108 SeqControl(7).command = 'loopCnt';
109 SeqControl(7).argument = numAvg-1;
110 SeqControl(8).command = 'jump';
111 SeqControl(8).argument = [];
112 SeqControl(9).command = 'loopTst';
113 SeqControl(9).argument = [];
114
115 nsc = 10;
116 j = 1;
117 m = 1;
118 for n = 1:Resource.RcvBuffer(1).numFrames
119     Event(j).info = 'Wait for trigger in';
120     Event(j).tx = 0;
121     Event(j).rcv = 0;
122     Event(j).recon = 0;
123     Event(j).process = 0;
124     Event(j).seqControl = 1;
125     j = j+1;
126
127     Event(j).info = 'noop and sync';
128     Event(j).tx = 0;
129     Event(j).rcv = 0;
130     Event(j).recon = 0;
131     Event(j).process = 0;
132     Event(j).seqControl = 5;
133     j = j+1;
134
135     Event(j).info = 'Acquire RF Data.';

```

```

136     Event(j).tx = 1;
137     Event(j).rcv = m;
138     Event(j).recon = 0;
139     Event(j).process = 0;
140     Event(j).seqControl = 6;
141     j = j+1;
142     m = m+1;
143
144     Event(j).info = 'Set loop count';
145     Event(j).tx = 0;
146     Event(j).rcv = 0;
147     Event(j).recon = 0;
148     Event(j).process = 0;
149     Event(j).seqControl = 7;
150     j = j+1;
151
152     Event(j).info = 'Jump to loop count test.';
153     Event(j).tx = 0;
154     Event(j).rcv = 0;
155     Event(j).recon = 0;
156     Event(j).process = 0;
157     Event(j).seqControl = 8;
158     j = j+1;
159
160     SeqControl(9).argument = j;
161
162     Event(j).info = 'Wait for trigger in';
163     Event(j).tx = 0;
164     Event(j).rcv = 0;
165     Event(j).recon = 0;
166     Event(j).process = 0;
167     Event(j).seqControl = 1;
168     j = j+1;
169
170     Event(j).info = 'noop and sync';
171     Event(j).tx = 0;
172     Event(j).rcv = 0;
173     Event(j).recon = 0;
174     Event(j).process = 0;
175     Event(j).seqControl = 5;
176     j = j+1;
177
178     Event(j).info = 'Acquire RF Data.';
179     Event(j).tx = 1;
180     Event(j).rcv = m;
181     Event(j).recon = 0;
182     Event(j).process = 0;
183     Event(j).seqControl = 6;
184     j = j+1;
185     m = m+1;
186
187     SeqControl(8).argument = j;
188
189     Event(j).info = 'Test loop count — if nz, jmp back to start of accumulates.';
190     Event(j).tx = 0;
191     Event(j).rcv = 0;
192     Event(j).recon = 0;
193     Event(j).process = 0;
194     Event(j).seqControl = 9;
195     j = j+1;
196
197     Event(j).info = 'Transfer data to host.';
198     Event(j).tx = 0;
199     Event(j).rcv = 0;
200     Event(j).recon = 0;
201     Event(j).process = 0;
202     Event(j).seqControl = 10;
203     SeqControl(10).command = 'transferToHost';
204     nsc = nsc+1;
205     j = j+1;
206
207     Event(j).info = 'Perform reconstruction and image display processing.';
208     Event(j).tx = 0;

```



```

209     Event(j).rcv = 0;
210     Event(j).recon = 0;
211     Event(j).process = 2; %set to 1 for frequency domain processing, to 2 for time domain
212     j = j+1;
213 end
214
215 Event(j).info = 'Jump back to Event 1.';
216 Event(j).tx = 0; % no TX structure.
217 Event(j).rcv = 0; % no Rcv structure.
218 Event(j).recon = 0; % no reconstruction.
219 Event(j).process = 0; % no processing
220 Event(j).seqControl = 3; % jump back to Event 1
221
222 % User Specified control elements
223 UI(1).Control = {'UserA2','Style','VsSlider','Label','Trig. delay ( s )',...
224 'SliderMinMaxVal',[135,300,180],...
225 'SliderStep',[0.01,0.1],'ValueFormat','%3.2f'};
226 UI(1).Callback = text2cell('%TrigDelayCallback');
227 UI(2).Control = {'UserB1','Style','VsPushButton','Label','Save'};
228 UI(2).Callback = text2cell('%ImSaveCallback');
229
230 EF(1).Function = vsv.seq.function.ExFunctionDef('rekon_OA_freqdom_LEGION', @
    rekon_OA_freqdom_LEGION);
231 EF(2).Function = vsv.seq.function.ExFunctionDef('PA_Reconstruct_DNS_LEGION', @
    PA_Reconstruct_DNS_LEGION);
232
233 save('MatFiles/IMA_C5-3_PA_standAlone.avg');
234 return
235 %% Callback routines
236 %TrigDelayCallback
237 SeqControl = evalin('base','SeqControl');
238 Resource = evalin('base','Resource');
239 for n = 5
240     SeqControl(n).command = 'triggerOut';
241     SeqControl(n).condition = 'syncNone';
242     SeqControl(n).argument = fix(UIValue)*250;
243 end
244 assignin('base','SeqControl',SeqControl);
245 Control = evalin('base','Control');
246 Control(1).Command = 'update&Run';
247 Control(1).Parameters = {'SeqControl'};
248 assignin('base','Control',Control);
249 return
250 %TrigDelayCallback
251
252 %ImSaveCallback
253 folder = ['IMA C5-3 Scripts\IMA_C5-3_PA_Data\' date '\'];
254 saveName = ['PA-' datestr(rem(now,1),'HH_MM_SS') '.mat'];
255 H = findobj('Type','Figure','Name','IMA_C5-3 PAI');
256 H = figure(H.Number);
257 ImageData = getimage(H);
258 XLim = H.CurrentAxes.XLim;
259 YLim = H.CurrentAxes.YLim;
260 if not(exist(folder) == 7)
261     mkdir(folder);
262 end
263 uisave({'ImageData','XLim','YLim'},[folder saveName]);
264 return
265 %ImSaveCallback
266
267 function rekon = rekon_OA_freqdom_LEGION(RData)
268 Resource = evalin('base','Resource');
269 DSrate = 1; %downsampling rate, speeds up reconstruction but loses quality
270 F = 20*DSrate; %sample frequency (MHz)
271 pitch = 0.3; % element pitch
272 c = Resource.Parameters.speedOfSound/1000;
273 delay = 0;
274 zeroX = 0;
275 zeroT = 0;
276 coeffT = 1;
277 samplingX = 1;
278 Mapping = dlmread('20180627 AMP128-18 channel map.csv',';',1,3); %
279 Mapping = [Mapping; Mapping+128];

```

```

280 RData = RData(1:DSrate:end,:)';
281 RDataRearranged = zeros(size(RData));
282 for n = 1:256
283     RDataRearranged(n,:) = RData(Mapping(n),:);
284 end
285 RData = RDataRearranged;
286
287 % signal data is transposed in order to fit to the algorithm
288 % which was initially implemented for element index
289 % corresponding to matrix lines
290
291 % ----- DATA DIMENSIONS -----
292 % dimension of the signal and image in number of samples
293 X = size(RData,1);
294 Z = size(RData,2);
295 T = Z;
296 % corresponding physical dimension of signal and image in [mm]
297 Xextent = X*pitch;
298 Zextent = Z*c/F;
299 Textent = T*c/F;
300 crossingpoint = Xextent/2;
301
302 xses = (1:X)*pitch - crossingpoint;
303 tses = (40.0/c)*(1-sqrt(1+((xses)/40.0).^2));
304 for lineind = 1:X
305     delayind = round(tses(lineind)*F);
306     RData(lineind,:) = circshift(RData(lineind,:),[0 -delayind]);
307 end
308 [kx,kz] = ndgrid([-ceil((X-1)/2):floor((X-1)/2)]/Xextent,...
309                 [-ceil((Z-1)/2):floor((Z-1)/2)]/Zextent);
310 kt = kz;
311
312 % 1D array containing values of kt
313 kate = [-ceil((Z-1)/2):floor((Z-1)/2)]/Zextent;
314 % maximum value of kt
315 katemax = ceil((Z-1)/2)/Zextent;
316 kt2 = -sqrt(kz.^2+kx.^2);
317 kt2(kz==0&&kx==0) = 1;
318 jakobiante = kz./kt2;
319 jakobiante(kz==0&&kx==0) = 1;
320 kt2(kz==0&&kx==0) = 0;
321 samplfreq = T/Textent;
322 kt2 = mod(kt2+samplfreq/2,samplfreq) - samplfreq/2;
323
324 sigtrans = fft2(RData);
325 sigtrans = fftshift(sigtrans);
326 sigtrans(kz>0) = 0;
327 ptrans = zeros(X,Z);
328 nTup = ceil((coeffT-1)/2);
329 nTdo = floor((coeffT-1)/2);
330 ktrange = -nTdo:nTup;
331 for xind = 1:X
332     ktind = round(kt2(xind,:)*Textent)+ ceil((T-1)/2) + 1;
333     ktind = ktind'*ones(1,coeffT) + ones(T,1)*ktrange;
334     ktind(ktind>T) = ktind(ktind>T)-T;
335     ktind(ktind<1) = ktind(ktind<1)+T;
336     V = sigtrans(xind + (ktind-1)*X);
337     Kt = kt(xind + (ktind-1)*X);
338     deltakt = kt2(xind,:)'*ones(1,coeffT) - Kt; % the distance between kt2 and kt
339     coeff = ones(T,coeffT); % prepare the coefficient matrix
340     help = deltakt~=0;
341     coeff(help) = (1 - exp(-2*pi*1i*deltakt(help)*Textent))./(...
342                 (2*pi*1i*deltakt(help)*Textent));
343
344     ptrans(xind,:) = sum(V.*coeff,2) .* jakobiante(xind,:);
345 end
346
347 ptrans(kt>0) = 0; % only negative kt are valid, 19/11/12
348
349 ptrans = ptrans.*exp(-2*pi*1i*kt2*delay*c);
350 ptrans = ptrans.*exp(2*pi*1i*kz*delay*c);
351
352 p = real(ifft2(ifftshift(ptrans)));

```

```

353 p(:,1:100) = 0;
354
355 rekon = abs(hilbert(p'));
356 H = findobj('Type','Figure','Name','IMA_C5-3 PAI');
357 figure(max(H.Number))
358 persistent RfHandle
359 if isempty(RfHandle) || ~ishandle(RfHandle)
360     RfHandle = H.Children;
361 end
362
363 xAx = linspace(-Xextent/2,Xextent/2,size(rekon,1));
364 zAx = linspace(0,Zextent,size(rekon,2));
365 imagesc(RfHandle,xAx,zAx,rekon)
366 daspect([1 1 1])
367 colorbar
368 drawnow
369 end
370
371 function PA_Reconstruct_DNS_LEGION(RData)
372 %% Initialisation , get Tx delay map from fit
373 Resource = evalin('base','Resource');
374 Fs = 20e6; %sample rate (Hz)
375 R = 40e-3; %array radius of curvature (m)
376 reconLat = 300*1e-6; %lateral pixel size
377 reconAx = 100*1e-6; %axial pixel size
378 startDepth = 0; %start depth in m
379 endDepth = 70e-3; %depth of image in total (m)
380 SoS = Resource.Parameters.speedOfSound;
381 zStep = SoS/Fs; %axial step size in RF data (m)
382 elementPitch = 0.3e-3;
383 xAxis = -127.5*elementPitch:reconLat:127.5*elementPitch;
384 zAxis = startDepth:reconAx:endDepth;
385 num_TimePoints = size(RData,1);
386 num_ScanElements = 256;
387 numLines = length(xAxis);
388 numPoints = length(zAxis);
389 elLatPos = R*sin((-127.5:127.5)*elementPitch/R); %lateral positions of elements
390 elAxPos = 2*R*sin((-127.5:127.5)*elementPitch/(2*R)).^2; %axial positions of elements
391 %rearrange RF data for LEGION amp, filter data
392 RDataRearranged = zeros(size(RData));
393 Mapping = dlmread('20180627 AMP128-18 channel map.csv',';',1,3);
394 Mapping = [Mapping; Mapping+128];
395 fcutlow=1e6;
396 fcuthigh=6.5e6;
397 [b,a]=butter(6,[fcutlow,fcuthigh]/(Fs/2),'bandpass');
398 for n = 1:256
399     RDataRearranged(:,n) = filter(b,a,RData(:,Mapping(n)));
400 end
401 RData = RDataRearranged;
402 %% Delay-and-sum section
403 BfData = zeros(numPoints,numLines);
404 SngIndMat = (ones(numPoints,1)*(0:numPoints:numPoints*numLines-1))'; %linear indexing of
    matrix
405 openingAngle = 30;%single detector element opening half-angle in degrees
406 for element = 1:num_ScanElements
407     Lmap = sqrt((ones(numPoints,1)*abs(xAxis - ones(1,numLines)*elLatPos(element))).^2 +
        ((zAxis-elAxPos(element))*ones(1,numLines)).^2);
408     l1 = Lmap.*(zInterface-elAxPos(element))./((zAxis-elAxPos(element))*ones(1,numLines)
        );
409     l2 = Lmap - l1;
410     indexMap = round(((l1/SoSint)+(l2/SoS))*Fs);
411     indexMap(indexMap > num_TimePoints) = num_TimePoints;
412     indexMap(indexMap == 0) = 1;
413     N = 1:numLines;
414     zStartInd = ones(numPoints,1)*floor((abs((N - element*(elementPitch/reconLat) + 1))*(
        elementPitch)/tand(openingAngle))/zStep);
415     direcMap = (indexMap > zStartInd);%account for directivity per element
416     for n = 1:numPoints+max(SngIndMat(:))
417         if direcMap(n) == 1
418             BfData(n) = BfData(n) + RData(indexMap(n),element);
419         end
420     end
421 end

```

```
422 %% Compound, display and save .fig and .txt
423 H = findobj('Type','Figure','Name','IMA-C5-3 PAI');
424 figure(max(H.Number))
425 persistent RfHandle
426 if isempty(RfHandle) || ~ishandle(RfHandle)
427     RfHandle = H.Children;
428 end
429 imagesc(RfHandle,1e3*xAxes,1e3*zAxes,abs(hilbert(BfData)))
430 daspect([1 1 1])
431 colorbar
432 drawnow
433 end
```

Appendix III. MATLAB-script for reconstructing the photoacoustic image.

```

1 %% PA_Reconstruct_C5_3_DNS.m
2 % David Thompson 04-05-2022
3 % Uses time-domain delay-and-sum algorithm to reconstruct photoacoustic images from
4 % curved C5-3 US probe
5 %
6 % Inputs:    double reconLatMicron - lateral pixel size of reconstructed image [ m ]
7 %           double reconAxMicron - axial pixel size of reconstructed image [ m ]
8 %           double latRange - lateral display range [mm] [minValue, maxValue]
9 %           double axRange - axial display range [mm] [minValue, maxValue]
10 %          double SoS - medium sound speed [m/s]
11 %          double SoSint - interface region sound speed [m/s] - only relevant if
12 %          there is an interface piece with a sound speed mismatch with
13 %          the phantom or medium being imaged
14 %          char filePath, path to the folder in which your RF data is saved
15 %
16 % Outputs:  Generates a figure, which is also saved in a .fig file
17 %           Saves a .txt file with reconstructed pixel values
18 %%
19 function PA_Reconstruct_C5_3_DNS(reconLatMicron, reconAxMicron, latRange, axRange, SoS, SoSint
    , filePath)
20 %open desired data - uses helper function opendata, should also be on path
21 [RfData, folder, fileName] = opendata(filePath, 'fileType', 'mat');
22 % average RF data
23 RfData = sum(RfData.RcvData{1}, 3) ./ size(RfData.RcvData{1}, 3);
24 % remap data because LEGION pre-amp used
25 RD_remapped = zeros(size(RfData));
26 channelMap = dlmread('20180627_AMP128-18_channel_map.csv', ';', 1, 3);
27 channelMap = [channelMap; channelMap+128];
28 for n = 1:256
29     RD_remapped(:, n) = RfData(:, channelMap(n));
30 end
31 RfData = RD_remapped;
32 %% Initialisation of variables
33 Fs = 20e6; %sample frequency
34 R = 40e-3; %probe radius of curvature
35 zInterface = 22e-3; %depth of interface piece (only relevant if SoSint /= SoS)
36 reconLat = reconLatMicron*1e-6;
37 reconAx = reconAxMicron*1e-6;
38 startDepth = 0; %start depth [m]
39 endDepth = 70e-3; %depth of image in total [m]
40 zStep = SoS/Fs; %axial step size [m]
41 elementPitch = 0.3e-3; %element pitch [m]
42
43 xAxis = -127.5*elementPitch:reconLat:127.5*elementPitch; %xAxis (lateral) for
    reconstructed data
44 zAxis = startDepth:reconAx:endDepth; %zAxis (axial) for reconstructed data
45 numTimePoints = size(RfData, 1);
46 numScanElements = 256;
47 numLines = length(xAxis);
48 numPoints = length(zAxis);
49 elLatPos = R*sin((-127.5:127.5)*elementPitch/R);
50 elAxPos = 2*R*sin((-127.5:127.5)*elementPitch/(2*R)).^2;
51 %% filter RF Data
52 fcutlow = 2e6;
53 fcuthigh = 6e6;
54 [b, a] = butter(6, [fcutlow, fcuthigh]/(Fs/2), 'bandpass');
55 for n = 1: 256
56     RfData(:, n) = filter(b, a, RfData(:, n));
57 end
58 %% Delay-and-sum section
59 BfData = zeros(numPoints, numLines);
60 SngIndMat = (ones(numPoints, 1)*(0:numPoints:numPoints*numLines-1))'; %linear indexing of
    matrix, suspect this can be rewritten in matrix form for improved efficiency
61 openingAngle = 30; %single detector element opening half-angle in degrees
62 N = 1:numLines;
63 tic
64 for element = 1:numScanElements
65     Lmap = sqrt((ones(numPoints, 1)*abs(xAxis - ones(1, numLines)*elLatPos(element))).^2 +
        ((zAxis - elAxPos(element))*ones(1, numLines)).^2);
66     ll = Lmap.*(zInterface - elAxPos(element))./((zAxis - elAxPos(element))*ones(1, numLines)
        );

```

```

67     l2 = Lmap - l1;
68     indexMap = round(((l1/SoSint)+(l2/SoS))*Fs);
69     indexMap(indexMap > num_TimePoints) = num_TimePoints;
70     indexMap(indexMap == 0) = 1;
71     zStartInd = ones(numPoints,1)*floor((abs((N - element*(elementPitch/reconLat) + 1))*(
        elementPitch)/tand(openingAngle))/zStep);
72     direcMap = (indexMap > zStartInd);%account for directivity per element
73     for n = 1:numPoints+max(SngIndMat(:))
74         if direcMap(n) == 1
75             BfData(n) = BfData(n) + RfData(indexMap(n),element);
76         end
77     end
78
79 end
80 toc
81 %% Envelope, display and save .fig and .txt
82 plotData = abs(hilbert(BfData));
83 figure;
84 saveIm = imagesc(1e3*xAxis,1e3*zAxis,plotData);
85 axis([latRange axRange])
86 daspect([1 1 1])
87 colormap hot
88 xlabel('x (mm)')
89 ylabel('z (mm)')
90 set(gca,'fontname','Corbel','fontsize',14)
91 colorbar
92 saveas(saveIm,[folder '\ ' fileName '_recon_' num2str(reconLatMicron) 'x' num2str(
        reconAxMicron) '_micronStep' num2str(SoS) 'mps.fig'])
93 % saveas(saveImLog,[folder '\ ' fileName '_recon_' num2str(reconLatMicron) 'x' num2str(
        reconAxMicron) '_micronStep_log_filt.fig'])
94 dlmwrite([folder '\ ' fileName '_recon_' num2str(reconLatMicron) 'x' num2str(reconAxMicron)
        ) '_micronStep_' num2str(SoS) 'mps.txt'],BfData);
95 %%
96 % cd C:\Users\ThompsonD\Documents\MATLAB

```

Appendix IV. MATLAB-script for obtaining the average PA signal of the ROI.

```

1  %{
2  This file collects the average PA value of a defined ROI for every measurement.
3  This is done by running the function RF_data_collector, which generates a
4  matrix for every measurement containing PA values for every pixel in the picture.
5  One set of measurement contains 40 files (5 concentrations, 8 wavelengths).
6  This script is now designed to do multiple sets of measurement. When one
7  set is done, adjust the first index (a) of the roi_value_test/ref and
8  average_roi_test/ref(a,i)
9
10 %}
11
12 %% Preallocating variables, run this section one time
13 num_files = 40;
14 roi_values_test = cell(6, num_files);
15 roi_values_ref = cell(6, num_files);
16 average_roi_test = zeros(6, num_files);
17 average_roi_ref = zeros(6, num_files);
18 x_length = 256;
19 y_length = 701;
20 [x, y] = meshgrid(1:x_length, 1:y_length);
21
22 %% Automatically select ROI and then calculate average signal
23 close all
24 [RF_data_norm, num_files] = RF_data_collector(300,100,[-30,30],[0,70],1485,1485);
25
26 %Define the region of interest. This script takes a circular ROI.
27
28 %X-value center of circle.
29 x_roi_center_test = 143;    %24 and 39 mm depth
30 x_roi_center_ref = 106;    %24 and 39 mm depth
31
32 %Y-value center of circle
33 y_roi_center = 246;        %24 mm depth
34 y_roi_center = 390;        %39 mm depth
35
36 radius = 16;
37
38 for i = 1:num_files
39     %ROI of test tube
40     roi_values_test{1,i} = RF_data_norm{i}(((x-x_roi_center_test).^2+(y-y_roi_center).^2)<=radius^2); %Taking only PA values of ROI
41     average_roi_test(1,i) = sum(sum(roi_values_test{1,i}))/numel(roi_values_test{1,i}); %Calculating average PA value in total ROI
42
43     %ROI of reference tube
44     roi_values_ref{1,i} = RF_data_norm{i}(((x-x_roi_center_ref).^2+(y-y_roi_center).^2)<=radius^2); %Taking only PA values of ROI
45     average_roi_ref(1,i) = sum(sum(roi_values_ref{1,i}))/numel(roi_values_ref{1,i}); %Taking only PA values of ROI
46
47     %To show the ROI of the test and reference tube in a photoacoustic image
48     if i == 1
49         roi_location = zeros(701, 256);
50         roi_location(((x-x_roi_center_test).^2+(y-y_roi_center).^2)<=radius^2)=10*10^4; %square ROI
51         roi_location(((x-x_roi_center_ref).^2+(y-y_roi_center).^2)<=radius^2)=10*10^4; %square ROI
52         figure();
53         RF_data_norm_img = RF_data_norm{i} + roi_location;
54         imagesc(RF_data_norm_img); %wrong image proportions, but correct for ROI selection.
55         xlabel('Pixel value'), ylabel('Pixel value')
56         title('Showing ROI selection')
57     end
58 end
59
60 %% PA vs wavelength, no compensation for one measurement
61 wavelengths = [680, 710, 740, 775, 795, 820, 850, 900]; %wavelengths measured,
62 adjust if necessary
63 figure(1)

```



```

64 plot(wavelengths, average_roi_test(4,1:8), 'Linewidth', 1.5)           %rows of
    average_roi_test determine the measurement, select the desired one.
65 hold on
66 plot(wavelengths, average_roi_test(4,9:16), 'Linewidth', 1.5)
67 hold on
68 plot(wavelengths, average_roi_test(4,17:24), 'Linewidth', 1.5)
69 hold on
70 plot(wavelengths, average_roi_test(4,25:32), 'Linewidth', 1.5)
71 hold on
72 plot(wavelengths, average_roi_test(4,33:40), 'Linewidth', 1.5)
73 hold on
74 title('Photoacoustic signal vs wavelength for 5 concentrations of India Ink at 39 mm
    depth','FontSize', 16)
75 xlabel('wavelength (nm)','FontSize', 16), ylabel('Photoacoustic signal (a.u.)','FontSize'
    , 16)
76 legend(' a = 0.391 India Ink', ' a = 0.529 India Ink', ' a = 0.814 India Ink', ' a =
    1.044 India Ink', ' a = 1.608 India Ink','FontSize', 14)
77 hold off

```

Appendix V. MATLAB-script for analysing the data and obtaining all the plots.

```

1 %% Analyse the PA signal from the test tube and make various plots
2 %{
3 In this script, multiple plots will be generated to analyse the data. To be
4 able to run the script, the following files have to be loaded:
5 00_average_roi_ref.mat, 00_average_roi_test.mat
6 These files contain the uncompensated average PA value of the ROI of all measurements for
  the
7 reference tube and the test tube, respectively.
8 This script consists of three parts. The first part compensate all the test tube signals
  for the reference tube.
9 The second and third part contain the same code, but the second part is
10 aimed at the analysis of the tubes located at 24 mm depth and the third part at the tubes
   located at 39 mm depth.
11 %}
12 %% Load constants, these are the known absorbance values and absorption coefficients
13 %%Every absorbance is concentration and wavelength dependend.
14 wavelengths = [680, 710, 740, 775, 795, 820, 850, 900];
15 Abs_500= [8.52, 8.1, 7.692, 7.308, 7.08, 6.84, 6.552, 6.144];
16 Mu_500 = log10(10.^Abs_500)/log10(exp(1))./10;
17 Abs_750 = [5.672, 5.4, 5.128, 4.864, 4.704, 4.544, 4.352, 4.04];
18 Mu_750 = log10(10.^Abs_750)/log10(exp(1))./10;
19 Abs_1000 = [4.116, 3.918, 3.732, 3.54, 3.426, 3.312, 3.168, 2.952];
20 Mu_1000 = log10(10.^Abs_1000)/log10(exp(1))./10;
21 Abs_1500 = [2.72, 2.592, 2.468, 2.336, 2.264, 2.176, 2.092, 1.968];
22 Mu_1500 = log10(10.^Abs_1500)/log10(exp(1))./10;
23 Abs_2000 = [2.088, 1.989, 1.893, 1.797, 1.74, 1.674, 1.608, 1.506];
24 Mu_2000 = log10(10.^Abs_2000)/log10(exp(1))./10;
25
26 %Computing the estimated absorption coefficient by using weight factors
27 for i = 1:6
28     wait_ref_500(i,:) = Mu_2000./ average_roi_ref(i,33:40); %ok<*SAGROW
29     >
30     wait_ref_750(i,:)= Mu_2000./ average_roi_ref(i,25:32);
31     wait_ref_1000(i,:)= Mu_2000./ average_roi_ref(i,17:24);
32     wait_ref_1500(i,:)= Mu_2000./ average_roi_ref(i,9:16);
33     wait_ref_2000(i,:)= Mu_2000./ average_roi_ref(i,1:8);
34
35     waited_test_500(i,:) = average_roi_test(i,33:40) .* wait_ref_500(i,:);
36     waited_test_750(i,:) = average_roi_test(i,25:32) .* wait_ref_750(i,:);
37     waited_test_1000(i,:) = average_roi_test(i,17:24) .* wait_ref_1000(i,:);
38     waited_test_1500(i,:) = average_roi_test(i,9:16) .* wait_ref_1500(i,:);
39     waited_test_2000(i,:) = average_roi_test(i,1:8) .* wait_ref_2000(i,:);
40 end
41 %making separeate matrices for the estimated mu_a values for every measurement
42 estimated_mu_24mm_1 = [waited_test_2000(1,:); waited_test_1500(1,:); waited_test_1000(1,:);
43     waited_test_750(1,:); waited_test_500(1,:)];
44 estimated_mu_24mm_2 = [waited_test_2000(2,:); waited_test_1500(2,:); waited_test_1000(2,:);
45     waited_test_750(2,:); waited_test_500(2,:)];
46 estimated_mu_24mm_3 = [waited_test_2000(3,:); waited_test_1500(3,:); waited_test_1000(3,:);
47     waited_test_750(3,:); waited_test_500(3,:)];
48 estimated_mu_39mm_1 = [waited_test_2000(4,:); waited_test_1500(4,:); waited_test_1000(4,:);
49     waited_test_750(4,:); waited_test_500(4,:)];
50 estimated_mu_39mm_2 = [waited_test_2000(5,:); waited_test_1500(5,:); waited_test_1000(5,:);
51     waited_test_750(5,:); waited_test_500(5,:)];
52 estimated_mu_39mm_3 = [waited_test_2000(6,:); waited_test_1500(6,:); waited_test_1000(6,:);
53     waited_test_750(6,:); waited_test_500(6,:)];
54 actual_mu = [Mu_2000; Mu_1500; Mu_1000; Mu_750; Mu_500];
55
56 %% showing reference signal after compensating with its own weight factors
57 %Reference signal without compensation
58 figure(1)
59 plot(wavelengths, average_roi_ref(1, 33:40), 'linewidth',1.5)
60 hold on
61 plot(wavelengths, average_roi_ref(1, 25:32), 'linewidth',1.5)
62 hold on
63 plot(wavelengths, average_roi_ref(1, 17:24), 'linewidth',1.5)
64 hold on
65 plot(wavelengths, average_roi_ref(1, 9:16), 'linewidth',1.5)
66 hold on
67 plot(wavelengths, average_roi_ref(1, 1:8), 'linewidth',1.5)

```

```

62 hold off
63 title('Average PA value from reference tube next to five different test tubes')
64 xlabel('wavelength (nm)'), ylabel('PA value (a.u.)')
65 legend('Next to test tube a = 0.391 India Ink', 'Next to test tube a = 0.529 India
        Ink', 'Next to test tube a = 0.814 India Ink', 'Next to test tube a = 1.044 India
        Ink', 'Next to test tube a = 1.608 India Ink')
66 hold off
67
68 %reference signal forced to absorption spectrum
69 figure(2)
70 plot(wavelengths, wait_ref_500(1,:).*average_roi_ref(1, 33:40), 'linewidth', 1.5)
71 hold on
72 plot(wavelengths, wait_ref_750(1,:).*average_roi_ref(1, 25:32), 'linewidth', 1.5)
73 hold on
74 plot(wavelengths, wait_ref_1000(1,:).*average_roi_ref(1, 17:24), 'linewidth', 1.5)
75 hold on
76 plot(wavelengths, wait_ref_1500(1,:).*average_roi_ref(1, 9:16), 'linewidth', 1.5)
77 hold on
78 plot(wavelengths, wait_ref_2000(1,:).*average_roi_ref(1, 1:8), 'linewidth', 1.5)
79 hold off
80 title('Reference tube forced to absorption spectrum')
81 xlabel('wavelength (nm)'), ylabel('Absorption coefficient \mu_a (mm^{-1})')
82 legend('Next to test tube a = 0.391 India Ink', 'Next to test tube a = 0.529 India
        Ink', 'Next to test tube a = 0.814 India Ink', 'Next to test tube a = 1.044 India
        Ink', 'Next to test tube a = 1.608 India Ink')
83 hold off
84
85 %test tube without compensating
86 figure(3)
87 plot(wavelengths, average_roi_test(1, 33:40), 'linewidth', 1.5)
88 hold on
89 plot(wavelengths, average_roi_test(1, 25:32), 'linewidth', 1.5)
90 hold on
91 plot(wavelengths, average_roi_test(1, 17:24), 'linewidth', 1.5)
92 hold on
93 plot(wavelengths, average_roi_test(1, 9:16), 'linewidth', 1.5)
94 hold on
95 plot(wavelengths, average_roi_test(1, 1:8), 'linewidth', 1.5)
96 hold off
97 title('Average PA value from different India Ink concentrations, not compensated')
98 xlabel('wavelength (nm)'), ylabel('PA value (a.u.)')
99 legend('a = 0.391 India Ink', 'a = 0.529 India Ink', 'a = 0.814 India Ink', 'a =
        1.044 India Ink', 'a = 1.608 India Ink')
100 hold off
101
102 %test tube compensated for differences in ref tube
103 figure(4)
104 plot(wavelengths, wait_ref_500(1,:).*average_roi_test(1, 33:40), 'linewidth', 1.5)
105 hold on
106 plot(wavelengths, wait_ref_750(1,:).*average_roi_test(1, 25:32), 'linewidth', 1.5)
107 hold on
108 plot(wavelengths, wait_ref_1000(1,:).*average_roi_test(1, 17:24), 'linewidth', 1.5)
109 hold on
110 plot(wavelengths, wait_ref_1500(1,:).*average_roi_test(1, 9:16), 'linewidth', 1.5)
111 hold on
112 plot(wavelengths, wait_ref_2000(1,:).*average_roi_test(1, 1:8), 'linewidth', 1.5)
113 hold off
114 title('Estimated \mu_a from different India Ink concentrations, compensated for reference
        tube')
115 xlabel('wavelength (nm)'), ylabel('Estimated \mu_a (mm^{-1})')
116 legend('a = 0.391 India Ink', 'a = 0.529 India Ink', 'a = 0.814 India Ink', 'a =
        1.044 India Ink', 'a = 1.608 India Ink')
117 hold off
118
119 %% Waiting test tube with wait factor from ref tube, to gain absorbance spectrum, 24 mm
        depth
120 %Plot compensated test tube over wavelength, average of all three measurements
121 figure(1);
122 %calculating the average PA value per wavelength for three measurements
123 all_2000_test = [waited_test_2000(1,:); waited_test_2000(2,:); waited_test_2000(3,:)];
124 err_2000 = std(all_2000_test); %calculating standard deviation.
125 avg_2000 = (waited_test_2000(1,:)+waited_test_2000(2,:)+waited_test_2000(3,:))/3;

```

```

126 errorbar(wavelengths, avg_2000, err_2000, '-o', 'linewidth', 1.5) %plot average PA value
    with errorbar
127 hold on
128
129 all_1500_test = [waited_test_1500(1,:);waited_test_1500(2,:); waited_test_1500(3,:)];
130 err_1500 = std(all_1500_test);
131 avg_1500 = (waited_test_1500(1,:)+waited_test_1500(2,:)+waited_test_1500(3,:))/3;
132 errorbar(wavelengths, avg_1500, err_1500, '-o', 'linewidth', 1.5)
133 hold on
134
135 all_1000_test = [waited_test_1000(1,:);waited_test_1000(2,:);waited_test_1000(3,:)];
136 err_1000 = std(all_1000_test);
137 avg_1000 = (waited_test_1000(1,:)+waited_test_1000(2,:)+waited_test_1000(3,:))/3;
138 errorbar(wavelengths, avg_1000, err_1000, '-o', 'linewidth', 1.5)
139 hold on
140
141 all_750_test = [waited_test_750(1,:);waited_test_750(2,:);waited_test_750(3,:)];
142 err_750 = std(all_750_test);
143 avg_750 = (waited_test_750(1,:)+waited_test_750(2,:)+waited_test_750(3,:))/3;
144 errorbar(wavelengths, avg_750, err_750, '-o', 'linewidth', 1.5)
145 hold on
146
147 all_500_test = [waited_test_500(1,:);waited_test_500(2,:);waited_test_500(3,:)];
148 err_500 = std(all_500_test);
149 avg_500 = (waited_test_500(1,:)+waited_test_500(2,:)+waited_test_500(3,:))/3;
150 errorbar(wavelengths, avg_500, err_500, '-o', 'linewidth', 1.5)
151 hold off
152 title('Estimated absorption coefficient vs wavelength for mutiple concentrations,
    compensated with weight factors from reference tube, 24 mm depth', 'FontSize', 20)
153 xlabel('wavelength (nm)', 'FontSize', 20), ylabel('Estimated absorption coefficient (mm
    -1)', 'FontSize', 20)
154 legend('a = 0.391 India Ink', 'a = 0.529 India Ink', 'a = 0.814 India Ink', 'a =
    1.044 India Ink', 'a = 1.608 India Ink', 'Exponential fit', 'FontSize', 20)
155
156 %Making exponential fit
157 log_2000 = log(avg_2000);
158 Prime_2000=polyfit(wavelengths,log_2000,1);
159 Prime_a_2000=Prime_2000(2);
160 Prime_b_2000=Prime_2000(1);
161
162 log_1500 = log(avg_1500);
163 Prime_1500=polyfit(wavelengths,log_1500,1);
164 Prime_a_1500=Prime_1500(2);
165 Prime_b_1500=Prime_1500(1);
166
167 log_1000 = log(avg_1000);
168 Prime_1000=polyfit(wavelengths,log_1000,1);
169 Prime_a_1000=Prime_1000(2);
170 Prime_b_1000=Prime_1000(1);
171
172 log_750 = log(avg_750);
173 Prime_750=polyfit(wavelengths,log_750,1);
174 Prime_a_750=Prime_750(2);
175 Prime_b_750=Prime_750(1);
176
177 log_500 = log(avg_500);
178 Prime_500=polyfit(wavelengths,log_500,1);
179 Prime_a_500=Prime_500(2);
180 Prime_b_500=Prime_500(1);
181
182 %Plot estimated mu_a and actual mu_a vs wavelength
183 figure(2)
184 plot(wavelengths, exp(Prime_a_2000)*exp(wavelengths*Prime_b_2000), '-*', 'Linewidth', 3)
185 hold on
186 plot(wavelengths, exp(Prime_a_1500)*exp(wavelengths*Prime_b_1500), '-*', 'Linewidth', 3)
187 hold on
188 plot(wavelengths, exp(Prime_a_1000)*exp(wavelengths*Prime_b_1000), '-*', 'Linewidth', 3)
189 hold on
190 plot(wavelengths, exp(Prime_a_750)*exp(wavelengths*Prime_b_750), '-*', 'Linewidth', 3)
191 hold on
192 plot(wavelengths, exp(Prime_a_500)*exp(wavelengths*Prime_b_500), '-*', 'Linewidth', 3)
193 hold on
194 plot(wavelengths, actual_mu, 'r-', 'Linewidth', 2)

```

```

195 hold off
196 ylim([0,2])
197 title('Estimated and actual absorption coefficient vs wavelength for mutliple
      concentrations, compensated with weight factors from reference tube, 24 mm depth', '
      Fontsize', 20)
198 xlabel('wavelength (nm)', 'Fontsize', 20), ylabel('Estimated absorption coefficient (mm
      -1)', 'Fontsize', 20)
199 legend(' a = 0.391 India Ink', ' a = 0.529 India Ink', ' a = 0.814 India Ink', ' a =
      1.044 India Ink', ' a = 1.608 India Ink', 'Actual a ', 'Fontsize', 20)
200
201 expfit_2000 = exp(Prime_a_2000)*exp(wavelengths*Prime_b_2000);
202 expfit_1500 = exp(Prime_a_1500)*exp(wavelengths*Prime_b_1500);
203 expfit_1000 = exp(Prime_a_1000)*exp(wavelengths*Prime_b_1000);
204 expfit_750 = exp(Prime_a_750)*exp(wavelengths*Prime_b_750);
205 expfit_500 = exp(Prime_a_500)*exp(wavelengths*Prime_b_500);
206
207 %Plot actual mu_a vs estimated mu_a
208 figure(3)
209 scatter(actual_mu(1,:), expfit_2000,140,'*','Linewidth', 1.5)
210 P_2000 = polyfit(actual_mu(1,:), expfit_2000,1);
211 yfit_2000 = polyval(P_2000, actual_mu(1,:));
212 hold on
213 plot(actual_mu(1,:), yfit_2000, '-.','Linewidth', 3);
214 hold on
215 eqn_2000 = string("Linear fit for \mu_a=0.391: y = " + P_2000(1)) + "x + " + string(
      P_2000(2));
216
217 scatter(actual_mu(2,:), expfit_1500,140,'*','Linewidth', 1.5)
218 P_1500 = polyfit(actual_mu(2,:), expfit_1500,1);
219 yfit_1500 = polyval(P_1500, actual_mu(2,:));
220 hold on
221 plot(actual_mu(2,:), yfit_1500, '-.','Linewidth', 3);
222 hold on
223 eqn_1500 = string("Linear fit for \mu_a=0.529: y = " + P_1500(1)) + "x + " + string(
      P_1500(2));
224
225 scatter(actual_mu(3,:), expfit_1000,140,'*','Linewidth', 1.5)
226 P_1000 = polyfit(actual_mu(3,:), expfit_1000,1);
227 yfit_1000 = polyval(P_1000, actual_mu(3,:));
228 hold on
229 plot(actual_mu(3,:), yfit_1000, '-.','Linewidth', 3);
230 hold on
231 eqn_1000 = string("Linear fit for \mu_a=0.814: y = " + P_1000(1)) + "x + " + string(
      P_1000(2));
232
233 scatter(actual_mu(4,:), expfit_750,140,'*','Linewidth', 1.5)
234 P_750 = polyfit(actual_mu(4,:), expfit_750,1);
235 yfit_750 = polyval(P_750, actual_mu(4,:));
236 hold on
237 plot(actual_mu(4,:), yfit_750, '-.','Linewidth', 3);
238 hold on
239 eqn_750 = string("Linear fit for \mu_a=1.044: y = " + P_750(1)) + "x + " + string(P_750
      (2));
240
241 scatter(actual_mu(5,:), expfit_500,140,'*','Linewidth', 1.5)
242 P_500 = polyfit(actual_mu(5,:), expfit_500,1);
243 yfit_500 = polyval(P_500, actual_mu(5,:));
244 hold on
245 plot(actual_mu(5,:), yfit_500, '-.','Linewidth', 3);
246 hold off
247 eqn_500 = string("Linear fit for \mu_a=1.608: y = " + P_500(1)) + "x + " + string(P_500
      (2));
248
249 xlim([0,2]), ylim([0,2])
250 legend('',eqn_2000, '',eqn_1500, '',eqn_1000, '', eqn_750, '', eqn_500, 'Fontsize', 18)
251 title('Actual vs estimated \mu_a for all five concentrations India Ink, Tubes located at
      24 mm depth', 'Fontsize', 20)
252 xlabel('Actual \mu_a (mm^{-1})', 'Fontsize', 20), ylabel('Estimated \mu_a (mm^{-1})', '
      Fontsize', 20)
253 slopes = [P_2000(1), P_1500(1), P_1000(1), P_750(1), P_500(1)];
254
255
256 conc = [0.391, 0.529, 0.814, 1.044, 1.608];

```

```

257 estimated_mu_680 = [avg_2000(1), avg_1500(1), avg_1000(1), avg_750(1), avg_500(1)];
258 estimated_mu_710 = [avg_2000(2), avg_1500(2), avg_1000(2), avg_750(2), avg_500(2)];
259 estimated_mu_740 = [avg_2000(3), avg_1500(3), avg_1000(3), avg_750(3), avg_500(3)];
260 estimated_mu_775 = [avg_2000(4), avg_1500(4), avg_1000(4), avg_750(4), avg_500(4)];
261 estimated_mu_795 = [avg_2000(5), avg_1500(5), avg_1000(5), avg_750(5), avg_500(5)];
262 estimated_mu_820 = [avg_2000(6), avg_1500(6), avg_1000(6), avg_750(6), avg_500(6)];
263 estimated_mu_850 = [avg_2000(7), avg_1500(7), avg_1000(7), avg_750(7), avg_500(7)];
264 estimated_mu_900 = [avg_2000(8), avg_1500(8), avg_1000(8), avg_750(8), avg_500(8)];
265
266 %exponential fit through data points of estimated mu_a values
267 log_680 = log(estimated_mu_680);
268 Prime_680=polyfit(conc, log_680, 1);
269 Prime_a_680=Prime_680(2);
270 Prime_b_680=Prime_680(1);
271
272 log_710= log(estimated_mu_710);
273 Prime_710=polyfit(conc, log_710, 1);
274 Prime_a_710=Prime_710(2);
275 Prime_b_710=Prime_710(1);
276
277 log_740= log(estimated_mu_740);
278 Prime_740=polyfit(conc, log_740, 1);
279 Prime_a_740=Prime_740(2);
280 Prime_b_740=Prime_740(1);
281
282 log_775= log(estimated_mu_775);
283 Prime_775=polyfit(conc, log_775, 1);
284 Prime_a_775=Prime_775(2);
285 Prime_b_775=Prime_775(1);
286
287 log_795= log(estimated_mu_795);
288 Prime_795=polyfit(conc, log_795, 1);
289 Prime_a_795=Prime_795(2);
290 Prime_b_795=Prime_795(1);
291
292 log_820= log(estimated_mu_820);
293 Prime_820=polyfit(conc, log_820, 1);
294 Prime_a_820=Prime_820(2);
295 Prime_b_820=Prime_820(1);
296
297 log_850= log(estimated_mu_850);
298 Prime_850=polyfit(conc, log_850, 1);
299 Prime_a_850=Prime_850(2);
300 Prime_b_850=Prime_850(1);
301
302 log_900= log(estimated_mu_900);
303 Prime_900=polyfit(conc, log_900, 1);
304 Prime_a_900=Prime_900(2);
305 Prime_b_900=Prime_900(1);
306
307 %Plot concentration vs estimated mu_a and concentration versus actual mu_a
308 figure(4)
309 scatter(conc, estimated_mu_680, '*', 'r')
310 hold on
311 plot(conc, exp(Prime_a_680)*exp(conc*Prime_b_680), 'r-', 'Linewidth', 3)
312 hold on
313
314 scatter(conc, estimated_mu_710, '*', 'g')
315 hold on
316 plot(conc, exp(Prime_a_710)*exp(conc*Prime_b_710), 'g-', 'Linewidth', 3)
317 hold on
318
319 scatter(conc, estimated_mu_740, '*', 'b')
320 hold on
321 plot(conc, exp(Prime_a_740)*exp(conc*Prime_b_740), 'b-', 'Linewidth', 3)
322 hold on
323
324 scatter(conc, estimated_mu_775, '*', 'c')
325 hold on
326 plot(conc, exp(Prime_a_775)*exp(conc*Prime_b_775), 'c-', 'Linewidth', 3)
327 hold on
328
329 scatter(conc, estimated_mu_795, '*', 'm')

```

```

330 hold on
331 plot(conc, exp(Prime_a_795)*exp(conc*Prime_b_795), 'm-', 'Linewidth', 3)
332 hold on
333
334 scatter(conc, estimated_mu_820, '*', 'y')
335 hold on
336 plot(conc, exp(Prime_a_820)*exp(conc*Prime_b_820), 'y-', 'Linewidth', 3)
337 hold on
338
339 scatter(conc, estimated_mu_850, '*', 'k')
340 hold on
341 plot(conc, exp(Prime_a_850)*exp(conc*Prime_b_850), 'k-', 'Linewidth', 3)
342 hold on
343
344 scatter(conc, estimated_mu_900, '*', 'r')
345 hold on
346 plot(conc, exp(Prime_a_900)*exp(conc*Prime_b_900), 'r-', 'Linewidth', 3)
347 hold on
348
349 plot(conc, actual_mu(:,1), '—r', 'Linewidth', 2)
350 hold on
351 plot(conc, actual_mu(:,2), '—g', 'Linewidth', 2)
352 hold on
353 plot(conc, actual_mu(:,3), '—b', 'Linewidth', 2)
354 hold on
355 plot(conc, actual_mu(:,4), '—c', 'Linewidth', 2)
356 hold on
357 plot(conc, actual_mu(:,5), '—m', 'Linewidth', 2)
358 hold on
359 plot(conc, actual_mu(:,6), '—y', 'Linewidth', 2)
360 hold on
361 plot(conc, actual_mu(:,7), '—k', 'Linewidth', 2)
362 hold on
363 plot(conc, actual_mu(:,8), '—r', 'Linewidth', 2)
364 hold off
365
366 %legend('For 680 nm light ', 'For 710 nm light ', 'For 740 nm light ', 'For 775 nm light ', 'For
      795 nm light ', 'For 820 nm light ', 'For 850 nm light ', 'For 900 nm light ', 'FontSize',
      20)
367 title('Concentration vs estimated and actual \mu_a for 8 wavelengths, 24 mm depth', '
      FontSize', 20)
368 xlabel('Concentration India Ink (\mu_a (mm^{-1}) for \lambda = 800 nm)', 'FontSize', 20)
369 ylabel('Estimated \mu_a', 'FontSize', 20)
370 legend(' ', 'Fitted curve for \lambda = 680 nm', ' ', 'Fitted curve for \lambda = 710 nm', ' ',
      'Fitted curve for \lambda = 740 nm', ' ', 'Fitted curve for \lambda = 775 nm', ' ', '
      Fitted curve for \lambda = 795 nm', ' ', 'Fitted curve for \lambda = 820 nm', ' ', '
      Fitted curve for \lambda = 850 nm', ' ', 'Fitted curve for \lambda = 900 nm', 'Actual \
      \mu_a vs concentration per \lambda', 'FontSize', 20)
371
372 %% 39 mm depth
373 %Plot compensated test tube versus wavelength, averaged over three
374 %measurements
375 figure(3);
376 all_2000_test = [waited_test_2000(4,:);waited_test_2000(5,:);waited_test_2000(6,:)];
377 err_2000 = std(all_2000_test); %calculating standard deviation.
378 avg_2000 = (waited_test_2000(4,:)+waited_test_2000(5,:)+waited_test_2000(6,:))/3;
379 errorbar(wavelengths, avg_2000, err_2000, '—o', 'linewidth', 1.5) %plot average PA value
      with errorbar
380 hold on
381
382
383 all_1500_test = [waited_test_1500(4,:);waited_test_1500(5,:);waited_test_1500(6,:)];
384 err_1500 = std(all_1500_test);
385 avg_1500 = (waited_test_1500(4,:)+waited_test_1500(5,:)+waited_test_1500(6,:))/3;
386 errorbar(wavelengths, avg_1500, err_1500, '—o', 'linewidth', 1.5)
387 hold on
388
389 all_1000_test = [waited_test_1000(4,:);waited_test_1000(5,:);waited_test_1000(6,:)];
390 err_1000 = std(all_1000_test);
391 avg_1000 = (waited_test_1000(4,:)+waited_test_1000(5,:)+waited_test_1000(6,:))/3;
392 errorbar(wavelengths, avg_1000, err_1000, '—o', 'linewidth', 1.5)
393 hold on
394

```



```

395 all_750_test = [waited_test_750(4,:);waited_test_750(5,:);waited_test_750(6,:)];
396 err_750 = std(all_750_test);
397 avg_750 = (waited_test_750(4,:)+waited_test_750(5,:)+waited_test_750(6,:))/3;
398 errorbar(wavelengths, avg_750, err_750, '-o', 'linewidth', 1.5)
399 hold on
400
401 all_500_test = [waited_test_500(4,:);waited_test_500(5,:);waited_test_500(6,:)];
402 err_500 = std(all_500_test);
403 avg_500 = (waited_test_500(4,:)+waited_test_500(5,:)+waited_test_500(6,:))/3;
404 errorbar(wavelengths, avg_500, err_500, '-o', 'linewidth', 1.5)
405 hold off
406 title('Estimated absorption coefficient vs wavelength for mutliple concentrations,
      compensated with weight factors from reference tube, 24 mm depth', 'FontSize', 20)
407 xlabel('wavelength (nm)', 'FontSize', 20), ylabel('Estimated absorption coefficient (mm
      -1)', 'FontSize', 20)
408 legend(' a = 0.391 India Ink', ' a = 0.529 India Ink', ' a = 0.814 India Ink', ' a =
      1.044 India Ink', ' a = 1.608 India Ink', 'Exponential fit', 'FontSize', 20)
409
410
411 %Exponential fit
412 wavelengths = [680, 710, 740, 775, 795, 820, 850, 900];
413 log_2000 = log(avg_2000);
414 Prime_2000=polyfit(wavelengths,log_2000,1);
415 Prime_a_2000=Prime_2000(2);
416 Prime_b_2000=Prime_2000(1);
417
418 log_1500 = log(avg_1500);
419 Prime_1500=polyfit(wavelengths,log_1500,1);
420 Prime_a_1500=Prime_1500(2);
421 Prime_b_1500=Prime_1500(1);
422
423 log_1000 = log(avg_1000);
424 Prime_1000=polyfit(wavelengths,log_1000,1);
425 Prime_a_1000=Prime_1000(2);
426 Prime_b_1000=Prime_1000(1);
427
428 log_750 = log(avg_750);
429 Prime_750=polyfit(wavelengths,log_750,1);
430 Prime_a_750=Prime_750(2);
431 Prime_b_750=Prime_750(1);
432
433 log_500 = log(avg_500);
434 Prime_500=polyfit(wavelengths,log_500,1);
435 Prime_a_500=Prime_500(2);
436 Prime_b_500=Prime_500(1);
437
438 %Plot estimated mu.a and actual mu.a versus wavelength
439 figure(2)
440 plot(wavelengths, exp(Prime_a_2000)*exp(wavelengths*Prime_b_2000), '-*', 'Linewidth', 3)
441 hold on
442 plot(wavelengths, exp(Prime_a_1500)*exp(wavelengths*Prime_b_1500), '-*', 'Linewidth', 3)
443 hold on
444 plot(wavelengths, exp(Prime_a_1000)*exp(wavelengths*Prime_b_1000), '-*', 'Linewidth', 3)
445 hold on
446 plot(wavelengths, exp(Prime_a_750)*exp(wavelengths*Prime_b_750), '-*', 'Linewidth', 3)
447 hold on
448 plot(wavelengths, exp(Prime_a_500)*exp(wavelengths*Prime_b_500), '-*', 'Linewidth', 3)
449 hold on
450 plot(wavelengths, actual_mu, 'r-', 'Linewidth', 2)
451 hold off
452 ylim([0,2])
453 title('Estimated and actual absorption coefficient vs wavelength for mutliple
      concentrations, compensated with weight factors from reference tube, 39 mm depth', '
      Fontsize', 20)
454 xlabel('wavelength (nm)', 'FontSize', 20), ylabel('Estimated absorption coefficient (mm
      -1)', 'FontSize', 20)
455 legend(' a = 0.391 India Ink', ' a = 0.529 India Ink', ' a = 0.814 India Ink', ' a =
      1.044 India Ink', ' a = 1.608 India Ink', 'Actual a', 'FontSize', 20)
456
457 expfit_2000 = exp(Prime_a_2000)*exp(wavelengths*Prime_b_2000);
458 expfit_1500 = exp(Prime_a_1500)*exp(wavelengths*Prime_b_1500);
459 expfit_1000 = exp(Prime_a_1000)*exp(wavelengths*Prime_b_1000);
460 expfit_750 = exp(Prime_a_750)*exp(wavelengths*Prime_b_750);

```

```

461 expfit_500 = exp(Prime_a_500)*exp(wavelengths*Prime_b_500);
462
463 %Plot actual mu_a versus estimated mu_a
464 figure(3)
465 scatter(actual_mu(1,:), expfit_2000,140,'*','Linewidth', 1.5)
466 P_2000 = polyfit(actual_mu(1,:), expfit_2000,1);
467 yfit_2000 = polyval(P_2000, actual_mu(1,:));
468 hold on
469 plot(actual_mu(1,:), yfit_2000, '-.','Linewidth', 3);
470 hold on
471 eqn_2000 = string("Linear fit for \mu_a=0.391: y = " + P_2000(1)) + "x + " + string(
    P_2000(2));
472
473 scatter(actual_mu(2,:), expfit_1500,140,'*','Linewidth', 1.5)
474 P_1500 = polyfit(actual_mu(2,:), expfit_1500,1);
475 yfit_1500 = polyval(P_1500, actual_mu(2,:));
476 hold on
477 plot(actual_mu(2,:), yfit_1500, '-.','Linewidth', 3);
478 hold on
479 eqn_1500 = string("Linear fit for \mu_a=0.529: y = " + P_1500(1)) + "x + " + string(
    P_1500(2));
480
481 scatter(actual_mu(3,:), expfit_1000,140,'*','Linewidth', 1.5)
482 P_1000 = polyfit(actual_mu(3,:), expfit_1000,1);
483 yfit_1000 = polyval(P_1000, actual_mu(3,:));
484 hold on
485 plot(actual_mu(3,:), yfit_1000, '-.','Linewidth', 3);
486 hold on
487 eqn_1000 = string("Linear fit for \mu_a=0.814: y = " + P_1000(1)) + "x + " + string(
    P_1000(2));
488
489 scatter(actual_mu(4,:), expfit_750,140,'*','Linewidth', 1.5)
490 P_750 = polyfit(actual_mu(4,:), expfit_750,1);
491 yfit_750 = polyval(P_750, actual_mu(4,:));
492 hold on
493 plot(actual_mu(4,:), yfit_750, '-.','Linewidth', 3);
494 hold on
495 eqn_750 = string("Linear fit for \mu_a=1.044: y = " + P_750(1)) + "x + " + string(P_750
    (2));
496
497 scatter(actual_mu(5,:), expfit_500,140,'*','Linewidth', 1.5)
498 P_500 = polyfit(actual_mu(5,:), expfit_500,1);
499 yfit_500 = polyval(P_500, actual_mu(5,:));
500 hold on
501 plot(actual_mu(5,:), yfit_500, '-.','Linewidth', 3);
502 hold off
503 eqn_500 = string("Linear fit for \mu_a=1.608: y = " + P_500(1)) + "x + " + string(P_500
    (2));
504
505 xlim([0,2]),ylim([0,2])
506 legend(' ',eqn_2000, ' ',eqn_1500, ' ',eqn_1000, ' ', eqn_750, ' ', eqn_500, 'FontSize', 18)
507 title('Actual vs estimated \mu_a for all five concentrations India Ink, Tubes located at
    39 mm depth', 'FontSize', 20)
508 xlabel('Actual \mu_a (nm^{-1})', 'FontSize', 20), ylabel('Estimated \mu_a (nm^{-1})', '
    FontSize', 20)
509 slopes = [P_2000(1), P_1500(1), P_1000(1), P_750(1), P_500(1)];
510
511
512 conc = [0.391, 0.529, 0.814, 1.044, 1.608];
513 estimated_mu_680 = [avg_2000(1), avg_1500(1), avg_1000(1), avg_750(1), avg_500(1)];
514 estimated_mu_710 = [avg_2000(2), avg_1500(2), avg_1000(2), avg_750(2), avg_500(2)];
515 estimated_mu_740 = [avg_2000(3), avg_1500(3), avg_1000(3), avg_750(3), avg_500(3)];
516 estimated_mu_775 = [avg_2000(4), avg_1500(4), avg_1000(4), avg_750(4), avg_500(4)];
517 estimated_mu_795 = [avg_2000(5), avg_1500(5), avg_1000(5), avg_750(5), avg_500(5)];
518 estimated_mu_820 = [avg_2000(6), avg_1500(6), avg_1000(6), avg_750(6), avg_500(6)];
519 estimated_mu_850 = [avg_2000(7), avg_1500(7), avg_1000(7), avg_750(7), avg_500(7)];
520 estimated_mu_900 = [avg_2000(8), avg_1500(8), avg_1000(8), avg_750(8), avg_500(8)];
521
522 %Exponential fit through data points of estimated mu_a
523 log_680 = log(estimated_mu_680);
524 Prime_680=polyfit(conc, log_680,1);
525 Prime_a_680=Prime_680(2);
526 Prime_b_680=Prime_680(1);

```

```

527
528 log_710= log(estimated_mu_710);
529 Prime_710=polyfit(conc,log_710,1);
530 Prime_a_710=Prime_710(2);
531 Prime_b_710=Prime_710(1);
532
533 log_740= log(estimated_mu_740);
534 Prime_740=polyfit(conc,log_740,1);
535 Prime_a_740=Prime_740(2);
536 Prime_b_740=Prime_740(1);
537
538 log_775= log(estimated_mu_775);
539 Prime_775=polyfit(conc,log_775,1);
540 Prime_a_775=Prime_775(2);
541 Prime_b_775=Prime_775(1);
542
543 log_795= log(estimated_mu_795);
544 Prime_795=polyfit(conc,log_795,1);
545 Prime_a_795=Prime_795(2);
546 Prime_b_795=Prime_795(1);
547
548 log_820= log(estimated_mu_820);
549 Prime_820=polyfit(conc,log_820,1);
550 Prime_a_820=Prime_820(2);
551 Prime_b_820=Prime_820(1);
552
553 log_850= log(estimated_mu_850);
554 Prime_850=polyfit(conc,log_850,1);
555 Prime_a_850=Prime_850(2);
556 Prime_b_850=Prime_850(1);
557
558 log_900= log(estimated_mu_900);
559 Prime_900=polyfit(conc,log_900,1);
560 Prime_a_900=Prime_900(2);
561 Prime_b_900=Prime_900(1);
562
563 %Plot concentration versus estimated mu_a and concentration versus actual
564 %mu_a
565 figure(4)
566 scatter(conc, estimated_mu_680, '*', 'r')
567 hold on
568 plot(conc, exp(Prime_a_680)*exp(conc*Prime_b_680), 'r-', 'Linewidth', 3)
569 hold on
570
571 scatter(conc, estimated_mu_710, '*', 'g')
572 hold on
573 plot(conc, exp(Prime_a_680)*exp(conc*Prime_b_710), 'g-', 'Linewidth', 3)
574 hold on
575
576 scatter(conc, estimated_mu_740, '*', 'b')
577 hold on
578 plot(conc, exp(Prime_a_740)*exp(conc*Prime_b_740), 'b-', 'Linewidth', 3)
579 hold on
580
581 scatter(conc, estimated_mu_775, '*', 'c')
582 hold on
583 plot(conc, exp(Prime_a_775)*exp(conc*Prime_b_775), 'c-', 'Linewidth', 3)
584 hold on
585
586 scatter(conc, estimated_mu_795, '*', 'm')
587 hold on
588 plot(conc, exp(Prime_a_795)*exp(conc*Prime_b_795), 'm-', 'Linewidth', 3)
589 hold on
590
591 scatter(conc, estimated_mu_820, '*', 'y')
592 hold on
593 plot(conc, exp(Prime_a_820)*exp(conc*Prime_b_820), 'y-', 'Linewidth', 3)
594 hold on
595
596 scatter(conc, estimated_mu_850, '*', 'k')
597 hold on
598 plot(conc, exp(Prime_a_850)*exp(conc*Prime_b_850), 'k-', 'Linewidth', 3)
599 hold on

```

```

600 scatter(conc, estimated_mu_900, '*', 'r')
601 hold on
602 plot(conc, exp(Prime_a_900)*exp(conc*Prime_b_900), 'r-', 'Linewidth', 3)
603 hold on
604
605
606 plot(conc, actual_mu(:,1), '—r', 'Linewidth', 2)
607 hold on
608 plot(conc, actual_mu(:,2), '—g', 'Linewidth', 2)
609 hold on
610 plot(conc, actual_mu(:,3), '—b', 'Linewidth', 2)
611 hold on
612 plot(conc, actual_mu(:,4), '—c', 'Linewidth', 2)
613 hold on
614 plot(conc, actual_mu(:,5), '—m', 'Linewidth', 2)
615 hold on
616 plot(conc, actual_mu(:,6), '—y', 'Linewidth', 2)
617 hold on
618 plot(conc, actual_mu(:,7), '—k', 'Linewidth', 2)
619 hold on
620 plot(conc, actual_mu(:,8), '—r', 'Linewidth', 2)
621 hold off
622
623 title('Concentration vs estimated and actual \mu_a for 8 wavelengths, 39 mm depth', '
        Fontsize', 20)
624 xlabel('Concentration India Ink (\mu_a (mm^{-1}) for \lambda = 800 nm)', 'Fontsize', 20)
625 ylabel('Estimated \mu_a', 'Fontsize', 20)
626 legend(' ', 'Fitted curve for \lambda = 680 nm', '', 'Fitted curve for \lambda = 710 nm', '
        ', 'Fitted curve for \lambda = 740 nm', '', 'Fitted curve for \lambda = 775 nm', '', '
        Fitted curve for \lambda = 795 nm', '', 'Fitted curve for \lambda = 820 nm', '', '
        Fitted curve for \lambda = 850 nm', '', 'Fitted curve for \lambda = 900 nm', 'Actual \
        \mu_a vs concentration per \lambda', 'Fontsize', 20)
627
628 %% Profile plots of three columns next to peak value
629 start_row = 385; %Start row, select region where the desired tube is located
630 start_col_test = 100;
631 for i = 1:40
632     region_test = RF_data_norm{i}(start_row:(start_row+30), start_col_test:(
        start_col_test+100));
633     [row_test(i), col_test(i)] = find(ismember(region_test, max(region_test(:))));
634     %row and column number for max intensity
        row_test(i) = row_test(i) + start_row -1;
        %compensating for
        start values
        col_test(i) = col_test(i) + start_col_test -1;
635 end
636
637
638 xaxis=(34:(8/70):42); %Set the x-axis to mm instead of
        pixels.
639
640 %Profile plots for the average PA signal from 3 columns. Region around the column and
        row that contain the maximum intensity of the tube.
641 %Figure 1 gives the profile plot for 1 concentration, all wavelengths.
642 last_file_wavelengths = 38; %Chose which data you want to investigate. Different
        files correspond to different measurements.
643 figure(1)
644 plot(xaxis, (sum(RF_data_norm{last_file_wavelengths-7,1}(row_test(
        last_file_wavelengths-7)-35:row_test(last_file_wavelengths-7)+35, col_test(
        last_file_wavelengths-7)-1:col_test(last_file_wavelengths-7)+1),2)/3), 'Linewidth
        ', 3) %Mu_a = 1.608; 900 nm
645 hold on
646 plot(xaxis, (sum(RF_data_norm{last_file_wavelengths-6,1}(row_test(
        last_file_wavelengths-6)-35:row_test(last_file_wavelengths-6)+35, col_test(
        last_file_wavelengths-6)-1:col_test(last_file_wavelengths-6)+1),2)/3), 'Linewidth
        ', 3) %Mu_a = 1.044; 900 nm
647 hold on
648 plot(xaxis, (sum(RF_data_norm{last_file_wavelengths-5,1}(row_test(
        last_file_wavelengths-5)-35:row_test(last_file_wavelengths-5)+35, col_test(
        last_file_wavelengths-5)-1:col_test(last_file_wavelengths-5)+1),2)/3), 'Linewidth
        ', 3) %Mu_a = 0.814; 900 nm
649 hold on
650 plot(xaxis, (sum(RF_data_norm{last_file_wavelengths-4,1}(row_test(
        last_file_wavelengths-4)-35:row_test(last_file_wavelengths-4)+35, col_test(

```

```

        last_file_wavelengths-4)-1:col_test(last_file_wavelengths-4)+1),2)/3), 'Linewidth
        ', 3)                %Mu_a = 0.529; 900 nm
651 hold on
652 plot(xaxis,(sum(RF_data_norm{last_file_wavelengths-3,1})(row_test(
        last_file_wavelengths-3)-35:row_test(last_file_wavelengths-3)+35, col_test(
        last_file_wavelengths-3)-1:col_test(last_file_wavelengths-3)+1),2)/3), 'Linewidth
        ', 3)                %Mu_a = 0.391; 900 nm, only showing the values of the rows
        around the tube
653 hold on
654 plot(xaxis,(sum(RF_data_norm{last_file_wavelengths-2,1})(row_test(
        last_file_wavelengths-2)-35:row_test(last_file_wavelengths-2)+35, col_test(
        last_file_wavelengths-2)-1:col_test(last_file_wavelengths-2)+1),2)/3), 'Linewidth
        ', 3)                %Mu_a = 0.391; 900 nm, only showing the values of the rows
        around the tube
655 hold on
656 plot(xaxis,(sum(RF_data_norm{last_file_wavelengths-1,1})(row_test(
        last_file_wavelengths-1)-35:row_test(last_file_wavelengths-1)+35, col_test(
        last_file_wavelengths-1)-1:col_test(last_file_wavelengths-1)+1),2)/3), 'Linewidth
        ', 3)                %Mu_a = 0.391; 900 nm, only showing the values of the rows
        around the tube
657 hold on
658 plot(xaxis,(sum(RF_data_norm{last_file_wavelengths-0,1})(row_test(
        last_file_wavelengths-0)-35:row_test(last_file_wavelengths-0)+35, col_test(
        last_file_wavelengths-0)-1:col_test(last_file_wavelengths-0)+1),2)/3), 'Linewidth',
        3)                %Mu_a = 0.391; 900 nm, only showing the values of the rows
        around the tube
659 hold off
660 title("PA value for average of 3 columns through centre of tube for 1.608 \mu_a India
        Ink, investigated for 8 wavelengths, 39 mm depth, one measurement", 'FontSize',
        20)
661 xlabel("Pixel on y-axis", 'FontSize', 20)
662 ylabel("Photoacoustic signal (a.u.)", 'FontSize', 20)
663 legend('680 nm', '710 nm', '740 nm', '775 nm', '795 nm', '820 nm', '850 nm', '900 nm'
        , 'FontSize', 20)
664 ylim([0,8*10^5]);
665
666 %Figure 2 gives profile plot for all concentrations, one wavelength.
667 %Last_file determines which wavelength
668 last_file_concentrations = 40;
669 figure(2)
670 plot(xaxis,(sum(RF_data_norm{last_file_concentrations-32,1})(row_test(
        last_file_concentrations-7)-35:row_test(last_file_concentrations-7)+35, col_test(
        last_file_concentrations-7)-1:col_test(last_file_concentrations-7)+1),2)/3), '
        Linewidth', 3)                %Mu_a = 1.608; 900 nm
671 hold on
672 plot(xaxis,(sum(RF_data_norm{last_file_concentrations-24,1})(row_test(
        last_file_concentrations-6)-35:row_test(last_file_concentrations-6)+35, col_test(
        last_file_concentrations-6)-1:col_test(last_file_concentrations-6)+1),2)/3), '
        Linewidth', 3)                %Mu_a = 1.044; 900 nm
673 hold on
674 plot(xaxis,(sum(RF_data_norm{last_file_concentrations-16,1})(row_test(
        last_file_concentrations-5)-35:row_test(last_file_concentrations-5)+35, col_test(
        last_file_concentrations-5)-1:col_test(last_file_concentrations-5)+1),2)/3), '
        Linewidth', 3)                %Mu_a = 0.814; 900 nm
675 hold on
676 plot(xaxis,(sum(RF_data_norm{last_file_concentrations-8,1})(row_test(
        last_file_concentrations-4)-35:row_test(last_file_concentrations-4)+35, col_test(
        last_file_concentrations-4)-1:col_test(last_file_concentrations-4)+1),2)/3), '
        Linewidth', 3)                %Mu_a = 0.529; 900 nm
677 hold on
678 plot(xaxis,(sum(RF_data_norm{last_file_concentrations-0,1})(row_test(
        last_file_concentrations-3)-35:row_test(last_file_concentrations-3)+35, col_test(
        last_file_concentrations-3)-1:col_test(last_file_concentrations-3)+1),2)/3), '
        Linewidth', 3)                %Mu_a = 0.391; 900 nm, only showing the values of the
        rows around the tube
679 hold on
680 title("PA signal value for sum of 3 columns through Peak value for five concentrations
        India Ink, \lambda = 820 nm, 39 mm depth, one measurement", 'FontSize', 20)
681 xlabel("Pixel on y-axis", 'FontSize', 20)
682 ylabel("Photoacoustic signal (a.u.)", 'FontSize', 20)
683 legend('a = 0.391 India Ink', 'a = 0.529 India Ink', 'a = 0.814 India Ink', 'a
        = 1.044 India Ink', 'a = 1.608 India Ink', 'FontSize', 20)
684 ylim([0,4*10^5]);

```